Clim. Past, 13, 795–818, 2017
https://doi.org/10.5194/cp-13-795-2017

Climate of the Past
Open Access
EGU

Palaeoclimate characteristics in interior Siberia of MIS 6–2: first insights from the Batagay permafrost mega-thaw slump in the Yana Highlands

Kseniia Ashastina[1,2], Lutz Schirrmeister[3], Margret Fuchs[4], and Frank Kienast[1]

[1]Senckenberg Research Institute and Natural History Museum, Research Station of Quaternary Palaeontology, Weimar, 99423, Germany
[2]Friedrich Schiller University Jena, Institute of Systematic Botany, Jena, 07743, Germany
[3]Alfred Wegener Institute Helmholtz Centre for Polar and Marine Research, Potsdam, 14471, Germany
[4]Helmholtz-Zentrum Dresden-Rossendorf, Helmholtz Institute Freiberg for Resource Technology, Freiberg, 09599, Germany

Correspondence to: Kseniia Ashastina (kseniia.ashastina@senckenberg.de)

Received: 2 August 2016 – Discussion started: 27 September 2016
Revised: 2 March 2017 – Accepted: 19 May 2017 – Published: 6 July 2017

Abstract. Syngenetic permafrost deposits formed extensively on and around the arising Beringian subcontinent during the Late Pleistocene sea level lowstands. Syngenetic deposition implies that all material, both mineral and organic, freezes parallel to sedimentation and remains frozen until degradation of the permafrost. Permafrost is therefore a unique archive of Late Pleistocene palaeoclimate. Most studied permafrost outcrops are situated in the coastal lowlands of northeastern Siberia; inland sections are, however, scarcely available. Here, we describe the stratigraphical, cryolithological, and geochronological characteristics of a permafrost sequence near Batagay in the Siberian Yana Highlands, the interior of the Sakha Republic (Yakutia), Russia, with focus on the Late Pleistocene Yedoma ice complex (YIC). The recently formed Batagay mega-thaw slump exposes permafrost deposits to a depth of up to 80 m and gives insight into a climate record close to Verkhoyansk, which has the most severe continental climate in the Northern Hemisphere. Geochronological dating (optically stimulated luminescence, OSL, and ^{14}C ages) and stratigraphic implications delivered a temporal frame from the Middle Pleistocene to the Holocene for our sedimentological interpretations and also revealed interruptions in the deposition. The sequence of lithological units indicates a succession of several distinct climate phases: a Middle Pleistocene ice complex indicates cold stage climate. Then, ice wedge growth stopped due to highly increased sedimentation rates and eventually a rise in temperature. Full interglacial climate conditions existed during accumulation of an organic-rich layer – plant macrofossils reflected open forest vegetation existing under dry conditions during Marine Isotope Stage (MIS) 5e. The Late Pleistocene YIC (MIS 4–MIS 2) suggests severe cold-stage climate conditions. No *alas* deposits, potentially indicating thermokarst processes, were detected at the site. A detailed comparison of the permafrost deposits exposed in the Batagay thaw slump with well-studied permafrost sequences, both coastal and inland, is made to highlight common features and differences in their formation processes and palaeoclimatic histories. Fluvial and lacustrine influence is temporarily common in the majority of permafrost exposures, but has to be excluded for the Batagay sequence. We interpret the characteristics of permafrost deposits at this location as a result of various climatically induced processes that are partly seasonally controlled. Nival deposition might have been dominant during winter time, whereas proluvial and aeolian deposition could have prevailed during the snowmelt period and the dry summer season.

1 Introduction

During Late Pleistocene marine regression stages, ice-rich deposits several dozen metres in thickness – the Yedoma Ice Complex (YIC), formed on the now-inundated Laptev and East Siberian Sea shelves and on the coastal lowlands of

northern Yakutia (Romanovskii et al., 2000a; Schirrmeister et al., 2013). Because they contain syngenetically frozen sediments and well-preserved fossil remains, YIC deposits provide a unique Late Pleistocene palaeoenvironmental archive. Due to their importance as sinks of organic carbon and as palaeoenvironmental archives, ice complex deposits have been of great scientific interest for decades (e.g. Kaplina, 1981; Giterman et al., 1982; Kienast et al., 2005; Sher et al., 2005; Walter et al., 2006; Strauss et al., 2013). Nevertheless, the main depositional processes that resulted in ice complex formation are still not yet fully understood and remain a subject of controversy (Schirrmeister et al., 2013; Murton et al., 2015). The concept of a purely aeolian origin of the mostly silty and fine-sandy, ice-rich deposits has become a widely accepted view in recent time (Zimov et al., 2012; Astakhov, 2014; Murton et al., 2015), but the assumption that loess covered the whole area during the Late Pleistocene contradicts cryolithological studies (Schirrmeister et al., 2011b). For this reason, the hypotheses of nival formation (Kunitsky, 1989), proluvial and slope genesis (Slagoda, 2004), and alluvial (Rozenbaum, 1981), or polygenetic genesis (Konishchev, 1981; Sher, 1997) are noteworthy.

YIC deposits in Yakutia are mainly accessible at natural outcrops along the sea coast or at river banks, primarily in the coastal lowlands; these areas are now under a certain influence of maritime climate, or a polar climate (ETf) according to Köppen (1884). However, this maritime climate influence was restricted to the time of sea level high stands during Quaternary warm stages. During cold stages, when the sea level was low, today's coastal sites were farther inland and under more continental climate influence. All discussed processes of YIC formation are either related to climate-dependent deposition (aeolian and nival processes) or to geomorphology (slope and alluvial deposition). To distinguish between aeolian and other processes in the resulting formation, the examination of YIC deposits in locations with climate and morphology differing from that in the northern coastal lowlands, i.e. more inland and in mountainous areas, is thought to contribute to a better understanding of the YIC genesis by comparing the lithological characteristics in different localities.

The Yana Highlands represent such a location because they form the benchmark for an inland climate north of the Arctic Circle. Verkhoyansk, located in the Yana Highlands, is recorded as the pole of cold; the Yana Highlands represent the region with the most severe climatic continentality in the Northern Hemisphere (Voeikov Main Geophysical Observatory, 1981; Harris et al., 2014). Kunitsky et al. (2013) reported on a rapidly proceeding permafrost thaw slump near Batagay, Verkhoyansky district, Sakha Republic (Yakutia), which has grown tremendously in the past 30–40 years. Due to thermo-denudation rates of up to 15 m per year, the mega-thaw slump reached a width of up to 800 m in 2014 (Günther et al., 2015). Situated in the Yana Highlands (Fig. 1), the Batagay exposure formed unaffected by fluvial or coastal abrasion processes. It is one of the few active permafrost out-

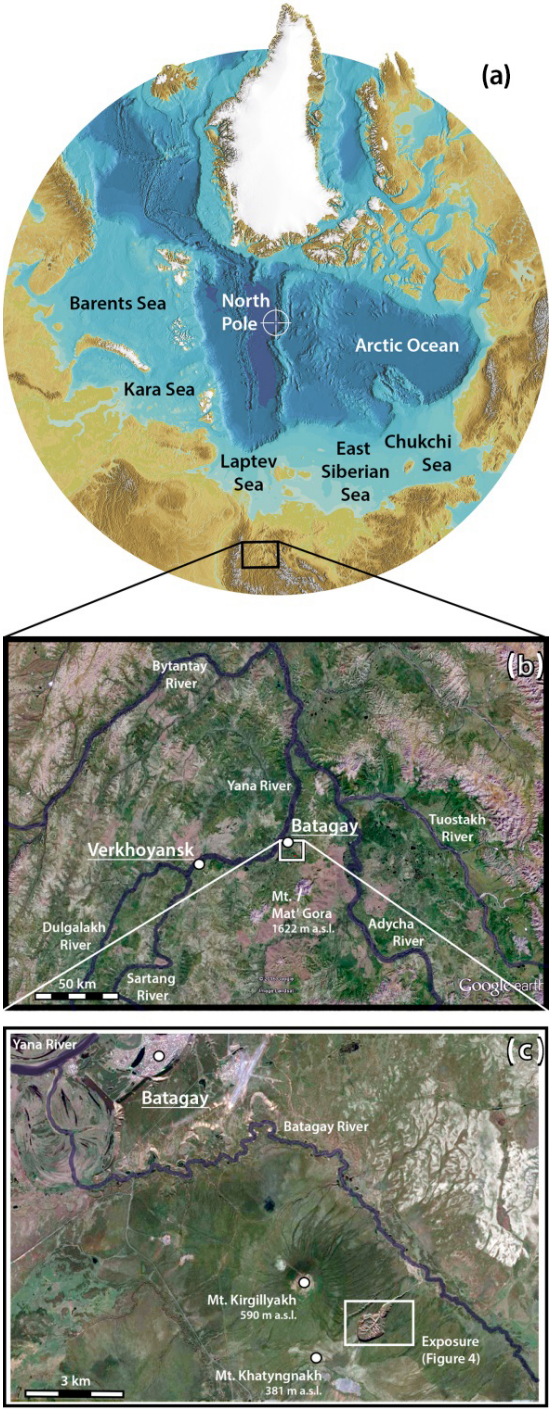

Figure 1. **(a)** Location of the Yana Highlands in northeastern Siberia. Map modified from the International Bathymetric Chart of the Arctic Ocean (Jakobsson, 2012). **(b)** Location of the study area on the right southeastern bank of the Yana River valley. **(c)** Location of the Batagay mega-slump (framed) at the northeastern slope of Mt. Khatyngnakh, left bank of the Batagay River. Panels **(b)** and **(c)** have been modified from satellite pictures, Google Earth 7.1.2.2041. Batagay region, Russia, 67°34′41.83″ N, 134°45′46.91″ E, 4 July 2013, viewed 25 April 2016, http://www.google.com/earth.

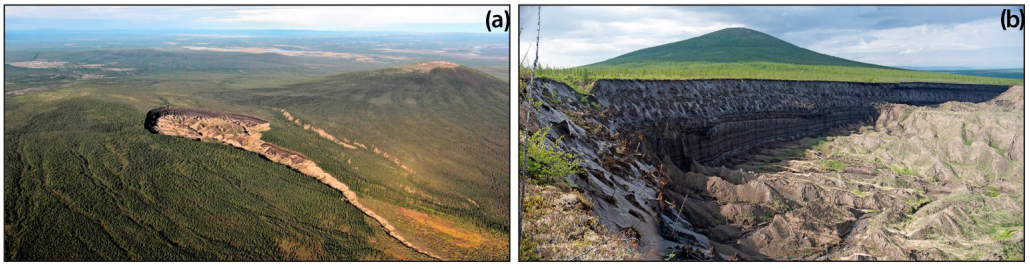

Figure 2. General views of the Batagay mega-slump. **(a)** From aircraft (L. Vdovina, Yana Geological Service, 17 August 2011). **(b)** The exposure at its deepest incision was photographed from the southern edge of the cirque (19 June 2014). For orientation, note Mt. Kirgillyakh in the upper right **(a)** or in the background **(b)**.

crops in interior Yakutia that exposes a long climate record of the Late Pleistocene or even older ages (Fig. 2).

Previous studies on the Batagay permafrost exposure reported on the structure and composition of the upper 12.5 m of the outcrop, discussed thermal denudation processes (Kunitsky et al., 2013), estimated expansion rates using remote sensing data (Günther et al., 2015), or described findings of mammoth faunal remains, including carcasses of horses (*Equus* sp.) and bison (*Bison priscus*), as well as bone remains of cave lions (*Panthera leo spelaea*), woolly rhinoceroses (*Coelodonta antiquitatis*), mammoths (*Mammuthus primigenius*), and other extinct Pleistocene animals (Novgorodov et al., 2013).

In this study, we describe the structural and sedimentological characteristics of the Batagay permafrost sequence. The main aims of our study are (i) to deduce a cryostratigraphical classification of this exceptional YIC sequence and its underlying units in comparison to other YIC records in northeastern Siberia, (ii) to differentiate the depositional processes and underlying climate conditions, and (iii) to highlight common features of and differences between coastal and inland YIC sequences in Yakutia to shed light on their formation processes and palaeoclimate history (Fig. 3).

2 Study site

The Batagay outcrop (67°34′41.83″ N, 134°45′46.91″ E) is located 10 km southeast of Batagay, the municipal centre of the Verkhoyansk district, Sakha Republic (Yakutia). The study site is located on the left bank of the Batagay River, a tributary to the Yana River, and descends down between 300 and 240 m a.s.l. into the foothills of Mt. Khatyngnakh, 381 m high (Fig. 1c). According to Günther et al. (2015), the height difference between the headwall and the outflow of the slump into the Batagay River is 145 m along a distance of 2300 m, while the maximum slump width is 800 m.

The study area belongs to the western side of the Verkhoyansk-Kolyma Orogen, which is characterized by the occurrence of Tertiary dark grey terrigenous siltstone (alevrolits) and argillite, mudstone that has undergone low-grade metamorphism (Vdovina, 2002; Fig. 3 geological map). Both siltstone and mudstone deposits contain layers of sands forming crumpled and broken sediment packs with intrusive rocks. In places, a weathered clayey crust covers the Neogene rocks. The Neogene is represented by clay deposits interspersed with pebbles and gravel, loam, sandy loam, and sands. Quaternary deposits are present as discontinuous layers covering older beds of hard rock and dispersed rocks (Kunitsky et al., 2013).

According to the climate classification of Köppen (1884), Batagay is characterized by a continental subarctic climate (Dfd). Continental climate is described by relatively low precipitation and a great seasonal (or in lower latitudes diurnal) temperature gradient forming under the influence of a large landmass and a great distance to the sea.

Meteorological observations recorded at the Verkhoyansk weather station continuously since 1888 revealed the greatest temperature range on earth. The mean July air temperature is accordingly +15.5 °C and the mean January air temperature is −44.7 °C. From an absolute winter minimum of −67.8 °C to the summer maximum of +37.3 °C, the temperature range equals 105.1 °C. The absolute winter minimum of −67.8 °C is accepted as the lowest temperature measured in the Northern Hemisphere (Lydolph, 1985; Ivanova, 2006). Verkhoyansk is therefore considered the northern pole of cold. The mean annual precipitation is only 181 mm, with the lowest rate during the winter (13 %) and the highest rate during the summer months (51 %) (USSR Climate Digest, 1989). In contrast, Ust-Yansk (70°55′ N, 136°26′ E) as an example of tundra climate (ET) in today's coastal zone, is characterized by a mean July temperature of +9.9 °C and a mean January temperature of −38.7 °C (https://de.climate-data.org/location/761428/). The seasonal temperature gradient is thus lower than inland. Annual precipitation equals 231 mm in the lowlands.

The location of the study area in the coldest part of the Northern Hemisphere is reflected by a mean annual ground temperature (MAGT) of −7.7 °C (Romanovsky et al., 2010) and a permafrost thickness of 300–500 m (Yershov and Williams, 2004). The permafrost formation, which started during the late Pliocene, was most likely influenced by local glaciers from the Chersky and Verkhoyansk moun-

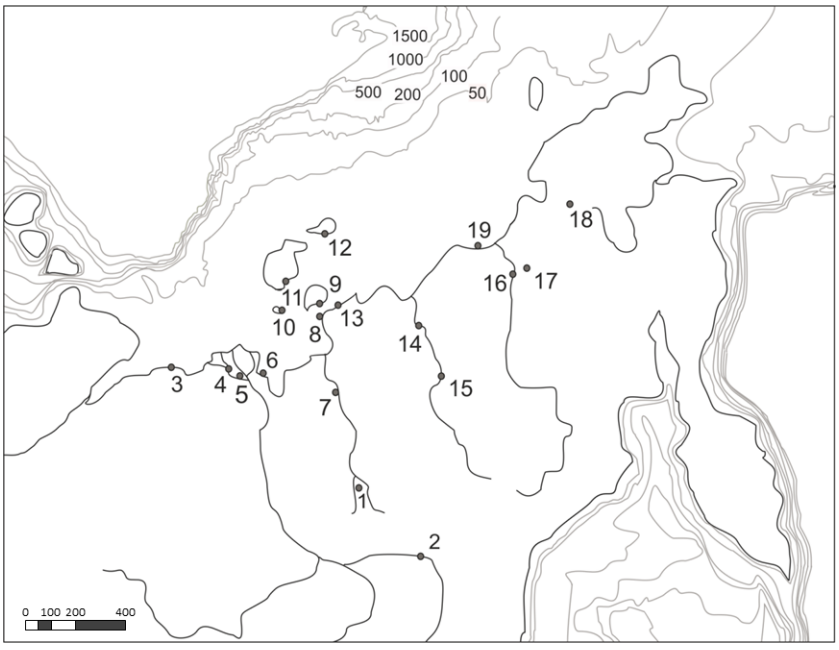

Figure 3. Overview map of the study region. Dots indicate sites mentioned in the text: 1 – Batagay outcrop, Yana Highlands; 2 – Mamontova Gora, Aldan River; 3 – Cape Mamotov Klyk, Laptev Sea; 4 – Diring Yuriakh Island, Lena Delta; 5 – Kurungnakh Island, Lena Delta; 6 – Bykovsky Peninsula, Laptev Sea; 7 – Mus-Khaya, Yana River; 8 – Cape Svyatoy Nos, Laptev Sea; 9 – Bol'shoy Lyakhovsky Island, New Siberian Archipelago; 10 – Stolbovoy Island, New Siberian Archipelago; 11 – Kotel'ny Island, New Siberian Archipelago; 12 – Island New Siberia, New Siberian Islands; 13 – Oyogos Yar, Dmitry Laptev Strait; 14 – Allaikha outcrop, Indigirka River; 15 – Sypnoy Yar, Indigirka River; 16 – Duvanny Yar, Kolyma River; 17 – Molotkovsky Kamen, Malyj Anjuy River; 18 – Lake El'gygytgyn; 19 – Chukochiy Yar, Chukochiy Cape. Combined and modified from Map of USSR, Main Bureau of Cartography and Geodesy, Moscow, 1958, pp. 3, 4, 8; the National Atlas of Russia, Volume 2, Main Bureau of Cartography and Geodesy, Moscow, 2004.

tains (Grinenko et al., 1998). Ice wedge casts in the Kutuyakh beds along the Krestovka River, northeastern Yakutia, indicate that permafrost already existed in northern Yakutia in the late Pliocene (Kaplina, 1981).

Similar to sites in the Yakutian coastal lowlands (Kaplina et al., 1980; Nikolskiy et al., 2010), thick YIC deposits also exist along the Aldan River in Central Yakutia (Markov, 1973; Péwé et al., 1977; Baranova, 1979; Péwé and Journaux, 1983) as well as in the valleys of the Yana Highlands (Katasonov, 2009; Kunitsky et al., 2013). As the result of intense thermal degradation, the Batagay mega-slump formed in just 40 years and cut about 60–80 m into ice-rich permafrost deposits (Kunitsky et al., 2013), dissecting them down to the bedrock at a depth of 110 m below ground surface (m b.g.s.) or 240 m above sea level (a.s.l.) (L. Vdovina, personal communication, 2014). A characteristic feature for the contact zone to the bedrock is the presence of cryogenic eluvium, frost weathering products of the siltstone that overlay leucogranite (alaskite).

The modern vegetation around the outcrop is light coniferous forest composed of larch (*Larix gmelinii*) and Siberian dwarf pine (*Pinus pumila*) as well as, in the shrub layer, *Salix spp.*, *Alnus fruticosa*, *Betula divaricata*, and *B. exilis*. Among dwarf shrubs, *Ledum palustre* and *Vaccinium vitis-idaea* are common. The ground is mostly wet and is densely covered with a thick layer of lichens and mosses, allowing only a few grasses and herbs to establish.

3 Methods

We described the Batagay permafrost sequence during the June 2014 field campaign. We used a Nikon D300 SLR camera to take photographs to be used for cryolithostratigraphical classifications. A Hama polarizing filter was used to highlight ground ice bodies for differentiating the cryolithological units. The 60 m high outcrop was sampled from top to bottom along its height, ideally in 1 m steps, but depending on its accessibility. The profile was sampled along three different transects: section A (0 to 10 m b.g.s.), section B (40 to 50 m b.g.s.), and section C (1 to 44 m b.g.s.) (Figs. 4, 5). Since the steep outcrop wall was not approachable due to the danger of falling objects along most of its length, samples were taken mainly from thermokarst mounds (*baidzherakhs*) in section C (Fig. 4b). The sampling procedure was carried out as follows: (1) the cryolithological characteristics at each sampling point were described and photographed, (2) the sampling zone was cleaned, and (3) frozen deposits were taken using a hammer and a chisel and placed into plas-

tic bags. The wet sediments were air-dried in the field and split into subsamples for sedimentological and biogeochemical analysis in the laboratories of the Alfred Wegener Institute in Potsdam.

Grain size analyses of the < 2 mm fraction were carried out using an LS 200 laser particle analyser (Beckman Coulter GmbH). Total carbon (TC) and total nitrogen (TN) were measured with a vario EL III element analyser and the total organic carbon (TOC) content was measured with a vario MAX analyser. Using the TOC and TN values, the TOC / TN (C / N) ratio was calculated to deduce the degree of organic matter decomposition. The lower the C / N ratio is, the higher the decomposition degree and vice versa (White, 2006; Carter and Gregorich, 2007). For TOC and stable carbon isotope (δ^{13}C) analyses, samples were decalcified for 3 h at 95 °C by adding a surplus of 1.3 N HCl. Total inorganic carbon (TIC) content was calculated by subtracting TOC from TC. Using TIC values, the carbonate content as $CaCO_3$ was estimated via the ratios of molecular weight. The δ^{13}C of TOC values was measured with a Finnigan Delta S mass spectrometer and expressed in delta per mil notation (δ, ‰) relative to the Vienna Pee Dee Belemnite (VPDB) standard with an uncertainty of 0.15‰. Variations in δ^{13}C values indicate changes in the local plant association and in the degree of organic matter decomposition (Hoefs and Hoefs, 1997). Lower δ^{13}C values correspond to less-decomposed organic matter, while higher δ^{13}C values reflect stronger decomposition (Gundelwein et al., 2007). Mass-specific magnetic susceptibility (MS) indicative of magnetic and magnetizable minerals was measured using Bartington MS2 instruments equipped with the MS2B sensor type. The data are expressed in 10–8 $m^3\ kg^{-1}$ (SI).

For accelerator mass spectrometry (AMS) radiocarbon dating in Poznan Radiocarbon Laboratory, Poland, we used terrestrial plant remains that had been identified (Table 2). No aquatic plant species were detected in the sampled material. Possible reservoir effects as a result of the accidental use of freshwater aquatics are thus eliminated. The AMS laboratory is equipped with the 1.5 SDH-Pelletron model "Compact Carbon AMS" serial no. 003 (Goslar et al., 2004). The results are presented in uncalibrated and calibrated ^{14}C years. The calibration was made with OxCal software (Bronk Ramsey, 2009) using IntCal 2013.

The lower part of the permafrost exposure was sampled for optically stimulated luminescence (OSL) dating. Two samples were taken in the form of cores from unfrozen but observably undisturbed deposits at the outer margin of thermokarst mounds. The tubes were sealed with opaque tape and transported to the OSL laboratory of TU Bergakademie Freiberg, Germany. One separate sediment sample was taken for high-purity germanium (HPGe) low-level gamma spectrometry in order to determine the radionuclide concentration required for dose rate calculations. OSL samples were treated under subdued red light. The outer 2 cm material layer was removed to retrieve only the inner core part that was not exposed to any light during sampling. The outer material was used for in situ water content measurements. The inner core part was processed for quartz and feldspar separation. Quartz procedures yielded sufficient material in the 90–160 µm as well as in the 63–100 µm fractions, while K-rich feldspar yielded only sufficient quantities for one sample in the 63–100 µm fraction. The chemical mineral separation and cleaning included the removal of carbonates (HCl 10 %) and organics (H_2O_2 30 %). The feldspar was separated from quartz using feldspar flotation (HF 0.2 %, pH 2.4–2.7, and dodecylamine). Subsequently, the density separation was performed to enrich K feldspars (2.53–2.58 g cm^{-3}) and quartz (2.62–2.67 g cm^{-3}). Quartz extracts were etched (HF 40 %) to remove the outer 10 µm of individual grains. After a final sieving, homogeneous sub-samples (aliquots) of quartz and K-feldspar extracts were prepared as a monograin layer on aluminium discs within a 2 mm diameter. OSL and infrared stimulated luminescence (IRSL) measurements were performed using a Risø TL/OSL Reader DA-20 (Bøtter-

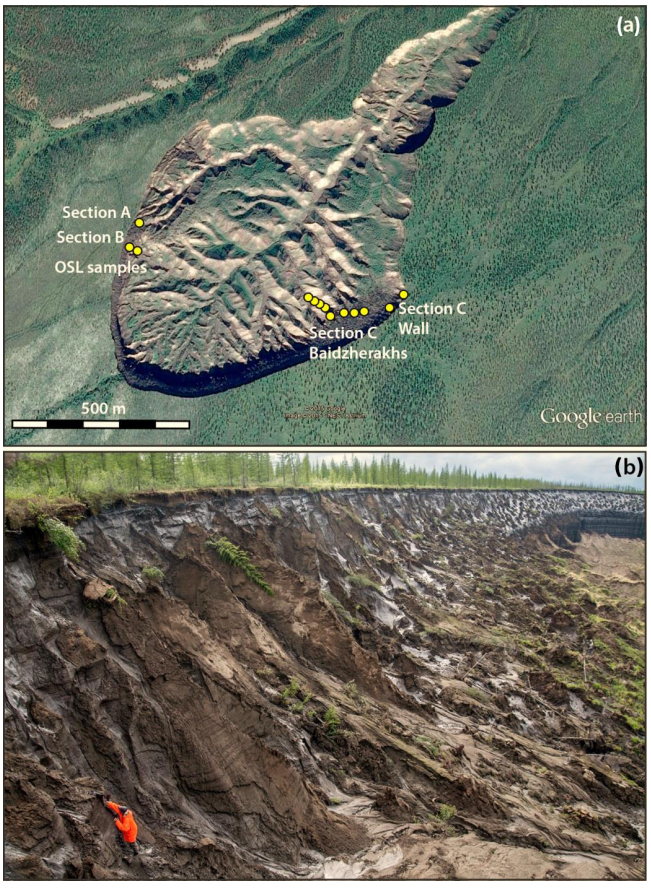

Figure 4. **(a)** Location of the studied sections in the Batagay mega-slump. Modified from Google Earth 7.1.2.2041. Batagay region, Russia, 67°34′41.83″ N, 134°45′46.91″ E, 4 July 2013, viewed 25 April 2016, http://www.google.com/earth. **(b)** Southeastern slope of the thaw slump, section C during sampling. Note person for scale.

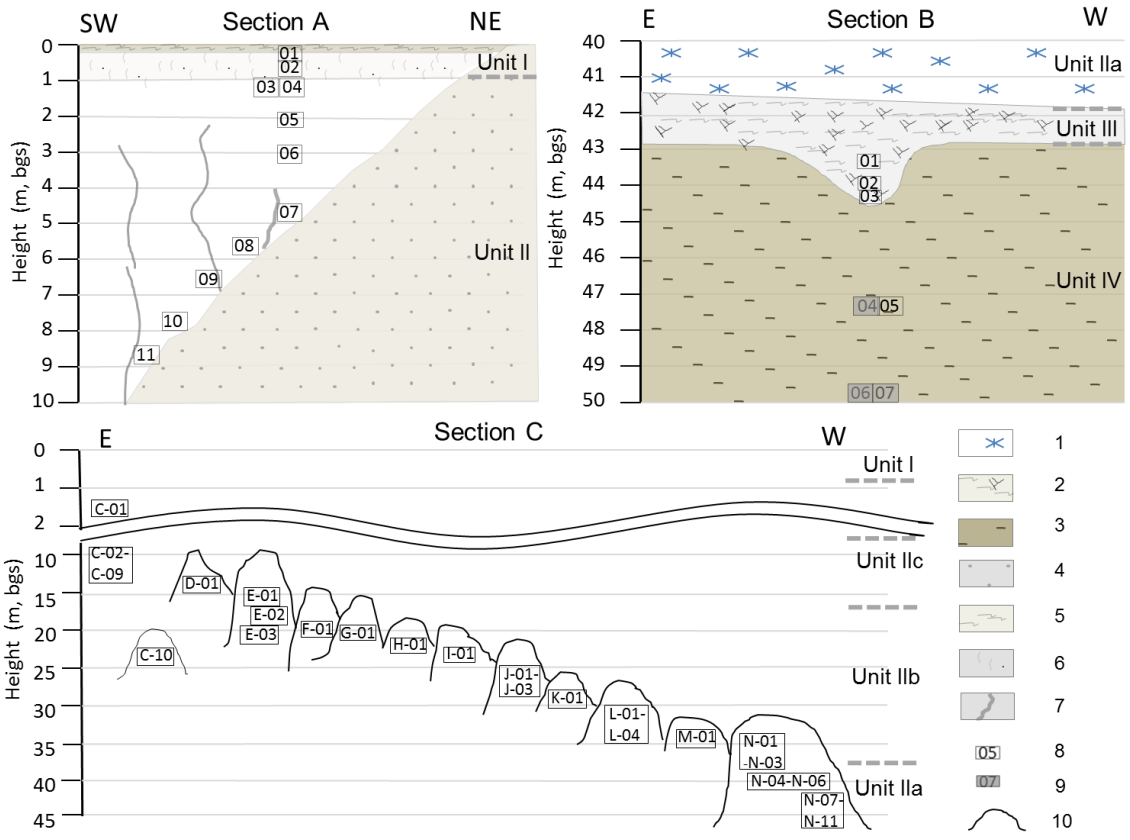

Figure 5. Sections of the Batagay permafrost exposure include the following: 1 – ice-rich sediments, 2 – organic layer with plant remains, 3 – layered cryostructure, 4 – sand, 5 – plant detritus, 6 – active layer with roots and coal, 7 – ice wedge, 8 – sediment and macrofossil sample site, 9 – OSL and sediment sample site, and 10 – *baidzherakh*.

Jensen et al., 2003) equipped with a 90 Sr beta irradiation source (4.95 Gy min^{-1}). Feldspar signal stimulation was performed at 870 nm with infrared diodes (125 °C for 100 s) and the emission was collected through a 410 nm optical interference filter to cut off scattered light from stimulation and was detected with a photomultiplier tube (Krbetschek et al., 1997). For quartz, blue LEDs of 470 nm were used for signal stimulation (125 °C for 100 s) and detection using a U 340 Hoya optical filter. Preheat and cut-heat temperatures were set to 240 and 200 °C, respectively. The measurement sequence followed the single-aliquot regenerative-dose (SAR) protocol according to Murray and Wintle (2000), including tests of dose recycling, recuperation, and correction for sensitivity changes. Appropriate measurement conditions were evaluated and adjusted based on preheat and dose-recovery tests (Murray and Wintle, 2003). Processing of measured data and statistical analyses were performed using the software Analyst v4.31.7 (Duller, 2015) and the R package "Luminescence" for statistical computing (Kreutzer et al., 2012). Sets of 10–40 equivalent doses for individual samples and grain size fractions were analysed for skewness and data scatter. To address sediment mixing that potentially affects permafrost sediments, age modelling was based on the central age model (CAM; Galbraith et al., 1999).

4 Results

4.1 Field observations and sampling

Differences in the thawing rates along the outcrop provide a variety of conditions on the bottom and along the margins of the thaw slump. The western, northwestern, and southwestern parts of the outcrop consist of nearly vertical walls that are eroding most actively (Fig. 6), while the southeastern side is a gentler slope with a gradient of up to 45° (Fig. 4b). Along the western and southern parts of the outcrop, meltwater and mud constantly flow off the steep slopes and form vertical drainage channels. The mud streams flowing downwards from the outcrop walls dissect a number of ridges up to 30 m high of frozen sediments on the bottom of the thermo-erosional gully, forming a fan that is visible in the satellite photo (Fig. 4a). Due to a slight northeastern inclination, the sediment-loaded meltwaters stream down to the Batagay River.

Table 1. Cryolithological description of the Batagay permafrost sequence.

Unit	Section	Observed depth (m b.g.s.)	Field description
I	A	0–0.09	Sod, no ice, composed mainly of modern plant litter including living plant parts.
		0.09–0.2	Light brown sediment with dusty structure. No ice. Horizon is penetrated by modern roots.
		0.20–0.43	Homogeneous light brown layer. No ice. Inclusions of oxidized iron and charcoal. Black spots 30-45 cm deep indicate relocation of solutes and incipient new mineral formation. The border to the underlying sediments is straight and horizontal.
		0.43–0.85	Brown horizon. No ice. Enriched with charcoal and modern plant roots.
	C	0.0–1.4	Silty sediments of dark grey colour, inclusions of charcoal.
		1.40	Top of an ice wedge. The border is clear with thaw unconformity.
II	A	0.85–4.0	Sandy silt in layered ice, layers of gravel, a few plant remains, and in situ rootlets.
		4.60–4.72	Reddish-coloured horizon with 8 cm wide ice veins crossing vertically. Rich in plant remains and contains an arctic ground squirrel burrow 0.2 × 0.12 m.
		5.0–5.8	Unstructured greyish sandy silt with abundant plant remains.
		5.8–6.5	Dark grey ice-rich sandy silt.
		6.5–9.5	Horizontal layers of greyish-brown sand (up to 7 cm thick) and ice bands (up to 5 cm thick); borders are well pronounced and sharp. No visible plant material.
	C	10.0	Sandy silt, horizontal layered ice bands. No visible plant material.
		16.5	Brownish-grey sandy silt, less ice-rich than above. Layered cryostructure. Inclusions of plant roots.
		19.5	Light brown horizon dissected by horizontal to sub-horizontal ice layers. Alternation of clayey and sandy layers with distinct wavy borders.
		22.0	Fulvous brown horizon with 1 mm thick ice veins.
		24.5	Homogeneous strata of greyish sediment structure and less ice. Distinct colour border with the underlying horizon. Layered cryostructure.
		32.0–32.5	Brownish-yellow horizon with abundant plant remains.
		32.5–37.0	Homogeneous strata of greyish sediment and horizontally layered ice bands.
		37.0–37.5	Alternation of grey and black layers, the latter with fulvous inclusions.
		37.5–43.5	Layered brown sediments in massive cryostructure. Clear border to the underlying unit.
III	B	40–42	Alternation of sandy silt layers with plant remains. Frozen organic sediments are extremely rich in large macroscopic plant remains, including numerous branches and twigs of woody plants. The layer with sharp boarders is visible along the wall of the outcrop. Thickness changes from 1 to 5 m filling former depressions that resemble ice wedge casts or small thermo-erosional drain channels. Pronounced erosional surface.
IV	B	42.0–50.0	Layered brown sands and narrow syngenetic ice wedges. Layered cryostructure.
V	Bottom in the central part of the thaw slump		Thick vertical ice wedges with truncated heads and dark layered sediment columns.

The outcropping sequence is composed of five visually distinct units with thicknesses changing along the outcrop (Fig. 6a). When the thickness of units is discussed, we refer to sections A and B unless otherwise stated (Fig. 6a–e, Table 1). Owing to the hillside location of the outcrop, the position of the ground surface differs between sections A and C and thus the depth below ground surface is only conditionally comparable between both sections.

A total of 11 radiocarbon dates are available for nine samples covering ages from modern to non-finite (Table 2). The OSL dating was applied to the lower sample available from Unit IV. Analytical sedimentological results are mainly available for Unit II and are summarized for sections A and B in Figs. 9 and 10 and for section C in Figs. 11 and 12.

4.2 Unit I

Unit I represents the active layer with a thickness varying from the southeast to the northwest wall of the exposure between 1.4 m b.g.s. and 0.85 m b.g.s., as measured at the end of June 2014. The well-bedded sandy sediments of Unit I were deposited in sub-layers 1–2 mm thick. The ≈ 9 cm thick modern vegetation sod is underlain by a homogeneous, brown to grey horizon containing numerous in-

Figure 6. The cryolithological structure of the Batagay exposure in its western and southwestern part. **(a)** General position of the detected cryolithological units (I to V). **(b)** Overall view of the outcrop. **(c)** Unit I (140 cm thick active layer) and boundary to Unit II (YIC) in section A. **(d)** Unit II, steep wall of the YIC illustrating the three observed subunits differing in ice content and contour. The trees as scale on top of the wall are about 6–8 m tall. Section A is situated at the upper part of the slope, on the right side of the photo. **(e)** Detail of the three lower cryolithological Units III, IV, and V. The old ice complex Unit V with preserved syngenetic ice wedges is only partly exposed.

Table 2. Radiocarbon dating results of the samples from the Batagay permafrost exposure. "Plant remains" stands for not identified remains of bark, twigs, and rootlets.

Lab. no.	Sample name	Depth [m b.g.s.]	Section/ unit	C [mg]	$\delta^{13}C$ (AMS)	Background pMC	Radiocarbon ages [ka BP]	Calibrated ages 2σ 95.4 % [cal ka BP]	Description
Poz-78149	19.6/A/4/1.15	1.15	A/I	1.5909	−27.3	0.29 ± 0.10	0.295 ± 0.03	0.459–0.347	Plant remains (twigs)
Poz-79751	19.6/A/5/2.05	2.05	A/IIc	2.4545	−25.1	0.25 ± 0.08	33.400 ± 0.5	37.305–38.259	Plant remains (twigs)
Poz-80390	19.6/A/5/2.05	2.05	A/IIc	1.7364	−24.6	0.29 ± 0.10	33.577 ± 472		Plant remains (twigs)
Poz-77152	20.6/A/1/460-472	4.6	A/IIc	0.7909	−24.8	0.30 ± 0.10	26.180 ± 0.22	28.965–27.878	*Plantago* sp., *Artemisia* sp., ground squirrel droppings
Poz-79756	22.6/C/2/8.5	8.5	C/IIc	2.2727	−24.3	–	12.660 ± 0.05	14.919–15.209	Plant remains (twigs)
Poz-79753	22.6/C/6/12.5	12.5	C/IIc	1.6818	−23.2	–	> 48.00		Plant remains (twigs)
Poz-79754	22.6/C/9/14.5	14.5	C/IIc	1.3049	−23.4	–	> 51.00		Plant remains (twigs)
Poz-79755	29.6/E/2/18.5	18.5	C/IIb	0.8864	−25.6	–	49.00 ± 2	51.034–52	*Papaver* sp.
Poz-78150	29.6/C/1/24.5	24.5	C/IIb	2.55	−23.2	–	110.31 ± 0.37pMC	1991 AD-2005 AD	*Alnus* sp., *Vaccinium vitis-idaea*
Poz-78878	29.6/C/1/24.5	24.5	C/IIb	1.5409	−29.6	0.35 ± 0.10	111.4 ± 0.37pMC		*Alnus* sp., *Vaccinium vitis-idaea*
Poz-66024	21.6/B/3/2	44	C/III	2.3092	−26.6	0.30 ± 0.10	> 49.00		Charcoal

clusions of charcoal and iron oxide impregnations (Fig. 7b). The upper part of the layer is penetrated by modern roots. The unit is homogenously light brown to brown in colour. The lower boundary of Unit I is separated sharply from the underlying Unit II (Fig. 7a).

One ^{14}C AMS date of 295 years BP is available from a sample taken directly above the permafrost table. No features of cryoturbation were observed but the horizon included roots of modern plants. The penetration of modern roots could be a reason for the modern date.

The unit is composed of 44–59 % fine sand with a mean grain size varying between 80 and 90 µm. The MS values are between 19 and 32 SI. The carbonate content is between 2.1 and 2.7 wt %. The TOC of the active layer was below the detection limit of 0.1 wt % in section A but about 1 wt % in

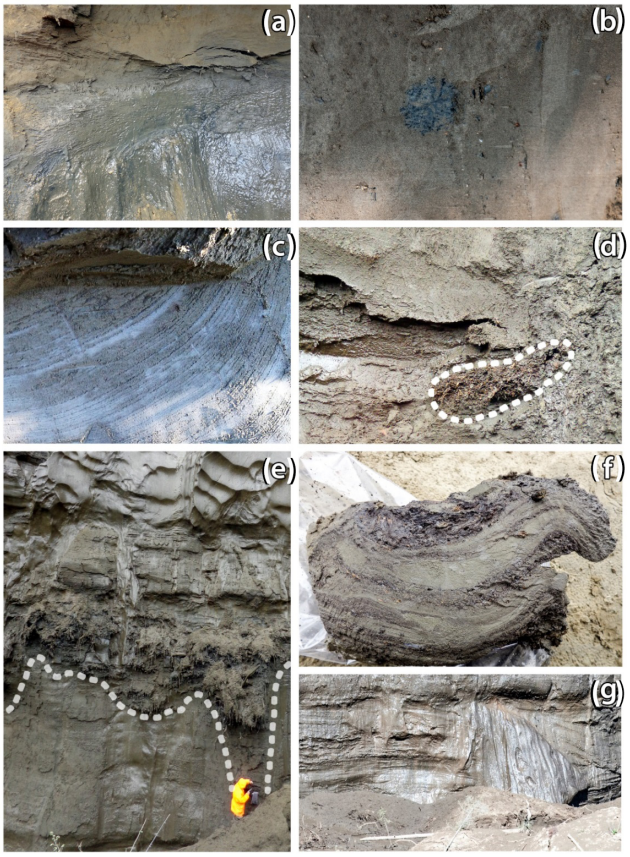

Figure 7. Typical sediment and cryostructures at the Batagay exposure. **(a)** Contact zone between the active layer, Unit I, and YIC, Unit II (section C). **(b)** Charcoal inclusions and iron oxide impregnations in Unit I (section A) at 0.20–0.43 m b.g.s. **(c)** Horizontally layered cryostructure of Unit II (section C). **(d)** Fossilized ground squirrel nest (dated ca 26 ka BP) at 4.7 m b.g.s. in Unit II (section A). **(e)** Organic-rich deposits filling a palaeo-depression ca. 42 m b.g.s. in section B; the person illustrates the position where sample no. 21.6/B/1/43 was taken. **(f)** Sample no. 21.6/B/1/43 in frozen state showing alternate bedding of sand and plant detritus layers. Thickness of the upper plant detritus layer is about 5 cm. **(g)** Ice-rich deposits in layered cryostructure enclosed by syngenetic ice wedges several metres thick in Unit V.

section C. The TN values are about 0.12 wt %. Because the TOC content was insufficient at < 0.1 wt %, $\delta^{13}C_{TOC}$ was not measurable and the C / N ratio could not be calculated.

4.3 Unit II

Unit II consists of the YIC, 30–40 m thick, composed of silty and sandy sediments in a layered cryostructure enclosed by syngenetic ice wedges, very narrow (0.08–0.2 m wide) in the northwestern part and ≤ 6 m wide in the western and southeastern parts of the exposure (Fig. 6b, d). Unit II can be described, according to unaided eye observations, as follows. The northwestern part of the YIC can be divided into three subunits that mainly differ in their ice contents; this difference results in unequal resistance to thermal erosion. Ice wedges gradually become more pronounced towards the top. The uppermost YIC subunit is stabilized by a massive ice wedge system resulting in a cliff overhang. Owing to less pronounced ice wedges and, as a result, increased thermal erosion, the middle subunit of Unit II is notched and forms a concave contour in the profile at the steepest point of the outcrop (Fig. 6d). The middle and upper subunits of Unit II are each about 8 m thick. This lower subunit of the YIC is the thickest of Unit II, reaching 20–25 m here. The southern part of unit II can also be visually divided into three subunits. Differences in ice content are not obviously prominent, but the contour of profile reveals an upper stratum and a lower stratum, each 8 m thick, and a middle, 20 m thick subunit. The deposits are characterized by grey to brown mineral-rich horizons, which alternate with thin ice-rich layers, 0.2 to 7 cm thick in layered cryostructure (Fig. 7c). The YIC deposits contain more or less evenly distributed organic material, mainly in the form of plant detritus and vertical roots of herbaceous plants. Occasionally, layers and patches with higher organic content can be found, e.g. a 0.2 m wide and 0.12 m thick brown fossilized ground squirrel nest with a high number of plant remains (Fig. 7d). The lower part of the Unit is composed of the layered brown sediments in massive cryostructure. The border to Unit III is distinct along the outcrop.

From Unit II, seven samples were radiocarbon dated. Three were double-checked and revealed similar ages. The dated plant taxa are available in Table 2. Material from 2.05 m b.g.s. in section A resulted in a date of 33 ± 0.5 ka BP, while plant material collected from a ground squirrel nest at 4.6 m b.g.s. in section A (Fig. 7c) revealed a ^{14}C AMS date of 26 ± 0.22 ka BP. In section C, dating results from 12.5 m and 14.5 m b.g.s. present non-finite ages of > 48 and > 51 ka BP, whereas plant material from 18.5 m b.g.s. was dated to 49 ± 2 ka BP.

In section C, we collected organic material with very well-preserved plant remains embedded in frozen ice-rich permafrost sediments. We assumed in situ preservation of old material in excellent condition. Dating of this sample, taken at a depth of 24.5 m b.g.s., revealed, however, that this material is of modern (1991–2005 AD) origin and was most likely eroded from the top and later refrozen in the wall.

The mean grain size of Unit II varies between 65 and 126 µm and is thus dominated by fine-grained sand. At about 30 m b.g.s., a distinct layer of medium-grained sand (mean diameter 253 µm) was detected. The MS values vary between 16 and 23 SI except for some higher values of 40, 31, and 43 SI at 43.5, 32.5, and 32 m b.g.s., respectively. The TOC ranges from < 0.1 to 4.8 wt %; higher values of ≥ 1 wt % were measured between 27.5 and 17.5 m b.g.s. in section C and 7.4 and 4.6 m b.g.s. in section A. The TN values range between < 0.1 and 0.49 wt %, while low TN values < 0.1 wt % are mostly accompanied by low TOC values. The C / N ratios

are mostly low and range from 2.4 to 9.8. Only one sample at a depth of 32.5 m b.g.s. shows a higher ratio of 13.1. The δ^{13}C values are rather uniformly distributed, ranging from −26.6 to −23.9 ‰ without any clear trend. The carbonate content is not stable within the profile and varies from 1.2 to 5.9 wt %, aside from one sample at 20.5 m b.g.s. with a lower carbonate content of 0.03 wt %. Comparing the fine-grained sand fraction data and TOC contents, Unit II in section C could be subdivided into three subunits (Figs. 8, 9). The lower part of Unit II between 43.5 and 34.5 m b.g.s. (Unit IIa) is dominated by fine-grained sand (> 50 %) with low TOC (< 0.1–0.7 wt %), whereas the middle part between 32.5 and 16.5 m b.g.s. (Unit IIb) contains less fine-grained sand (20–50 %) and a higher TOC content (0.7–4.8 wt %). The upper subunit at a depth from 16.5 to 8.5 m b.g.s. (Unit IIc) is again mainly composed of fine-grained sand with low TOC.

4.4 Unit III

Unit III consists of frozen sediments that are rich in large macroscopic plant remains, including numerous branches and twigs of woody plants. Situated directly below the YIC, this horizon is detectable over the whole distance of the outcrop, mostly as a relatively thin layer of estimated ≈ 1.5 m thickness sharply delineated from the YIC and Unit IV (Fig 6a, e). In several places, however, there exist accumulations of Unit III organic matter ≈ 5 m thick filling former depressions that resemble ice wedge casts or small thermo-erosional drain channels (Figs. 7e, 8b). Unit III was sampled in the lower part of such a pocket-like accumulation below the coarse woody layer at a depth of about 40 to 44 m b.g.s. The samples taken in section B consist of organic material, including numerous seeds, fruits, and plant debris in a distorted fine bedding alternating with silty fine sand beds (Fig. 7f). Plant macrofossil analyses detected numerous taxa characteristic of northern taiga forests as they occur today at the study site. The main components of the reconstructed vegetation were larch (*Larix gmelinii*) as well as birch (*Betula* spp.) and shrub alder (*Alnus fruticosa*). No aquatic plant taxa were detected.

The erosional surface is pronounced. One sample from Unit III was taken for ^{14}C AMS dating from the lower part of a sediment-filled depression about 6 m below Unit II in section B at a depth of 44 m b.g.s. The dating resulted in an infinite age of > 44 ka BP.

The sedimentological characteristics of the lowermost part of Unit III were studied in section B with two samples from depths of 43 and 44 m b.g.s. (Figs. 7f, 11, 12). The major fraction in the grain size distribution (GSD) of Unit III is fine-grained sand, accounting for 41–45 %. MS equals 30 SI. The TOC values are ≈ 3.3 wt %, the C / N ratio is ≈ 13, the δ^{13}C values range from −26.5 to −26.1 ‰, and the carbonate content is 2.5–2.8 wt %.

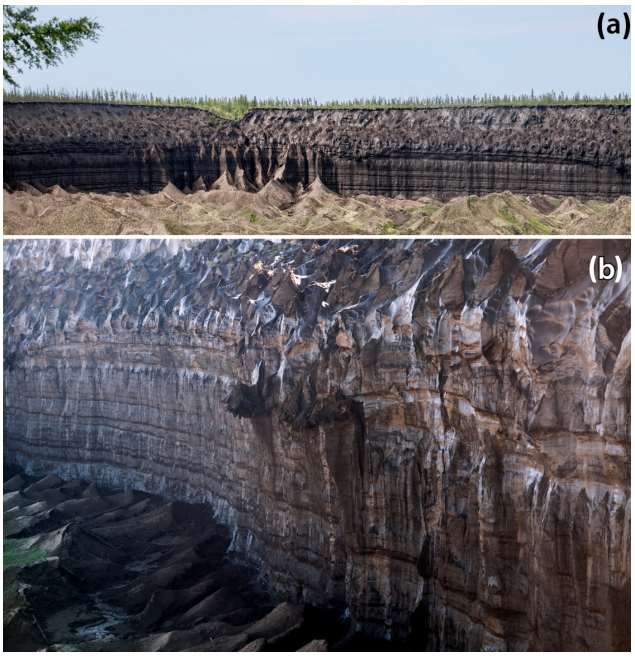

Figure 8. **(a)** Total view of the southwestern part of the outcrop showing that the sequence continues homogeneously over large distances. In the left central part of the photo, note the section of an erosional channel visible in the bottom-left corner of the satellite picture in Fig. 4a. For scale: the trees on top of the profile are on average about 7 m tall. **(b)** Detail of the profile illustrating stratification and borders between Units II, III, IV, and V. Also, it is shown that accumulations of organic material in Unit III occur at isolated places but not as a recurring pattern as would be assumed for fills of ice wedge casts penetrating Unit IV. Instead, they might represent ancient depressions such as transects of channels resembling the modern one in Fig. 8a.

4.5 Unit IV

Unit IV, which reaches a thickness of ≈ 25 m, almost reaches to the bottom of the exposure in most places. Unit IV is composed of distinct horizontally layered frozen sediments (Fig. 6a, e) that are traceable without interruption over large distances along the steepest part of the outcrop (Fig. 6b). Unit IV is separated sharply from the overlying Unit III (Fig. 6e). The border to Unit V is distinct in colour: brown in Unit IV and dark grey in Unit V. In contrast to the YIC, Unit IV is neither penetrated by wide ice wedges, nor does it contain regular ice wedge casts. Its cryostructure is layered: sediment beds are 5–20 cm thick and separated by ice layers. Exposed exclusively at the steepest part of the profile, Unit IV was not accessible for orderly sampling due to the danger of objects frequently falling from the > 60 m high, intensely thawing and eroding, partly overhanging permafrost wall. Only one sample was collected in situ from a ridge of frozen deposits in 50 m b.g.s. for OSL dating and sedimentological analyses. According to the sedimentological characteristics of this material, Unit IV clearly differs from the

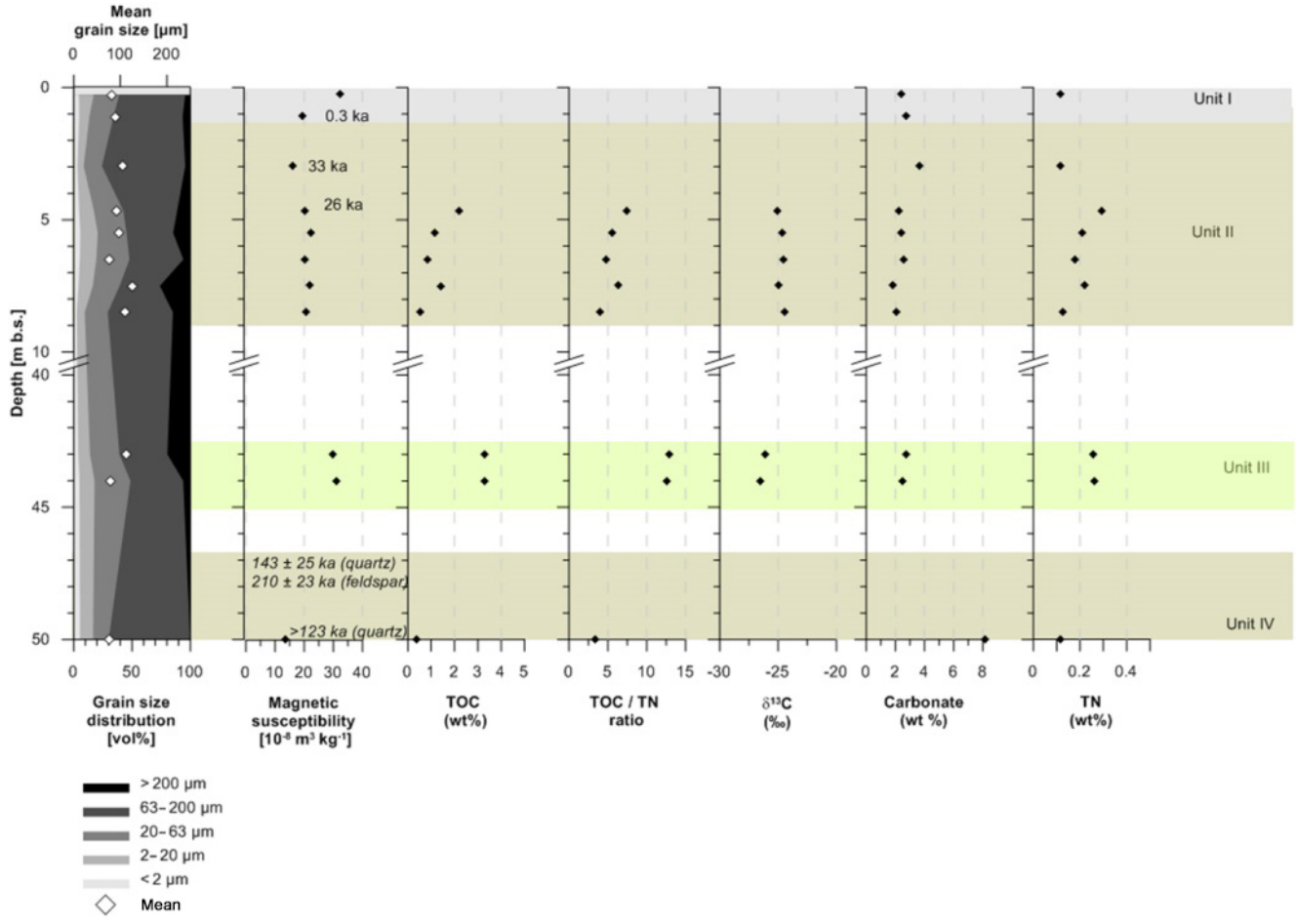

Figure 9. Diagram presenting grain size distribution, MS, TOC and TOC / TN, $\delta^{13}C$, and carbonate records for section A.

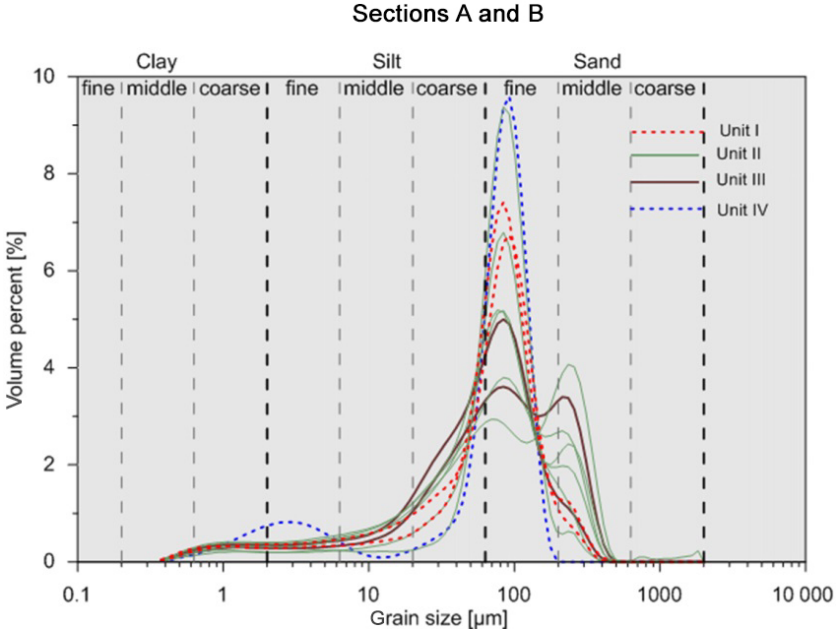

Figure 10. Grain size distribution plot for sections A and B of the Batagay permafrost outcrop.

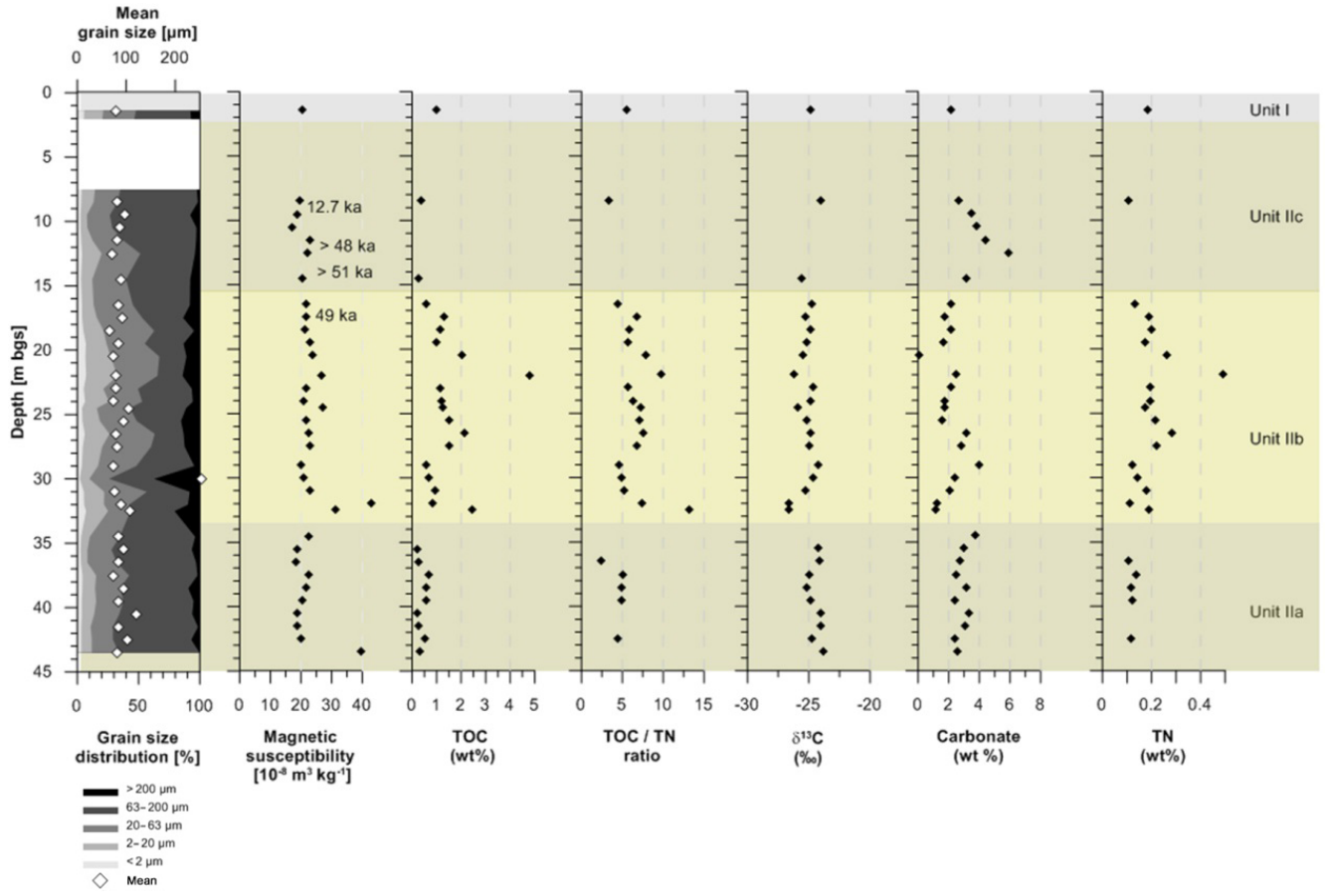

Figure 11. Diagram presenting grain size distribution, MS, radiocarbon ages, TOC, TOC / TN, δ^{13}C, and carbonate records for section C.

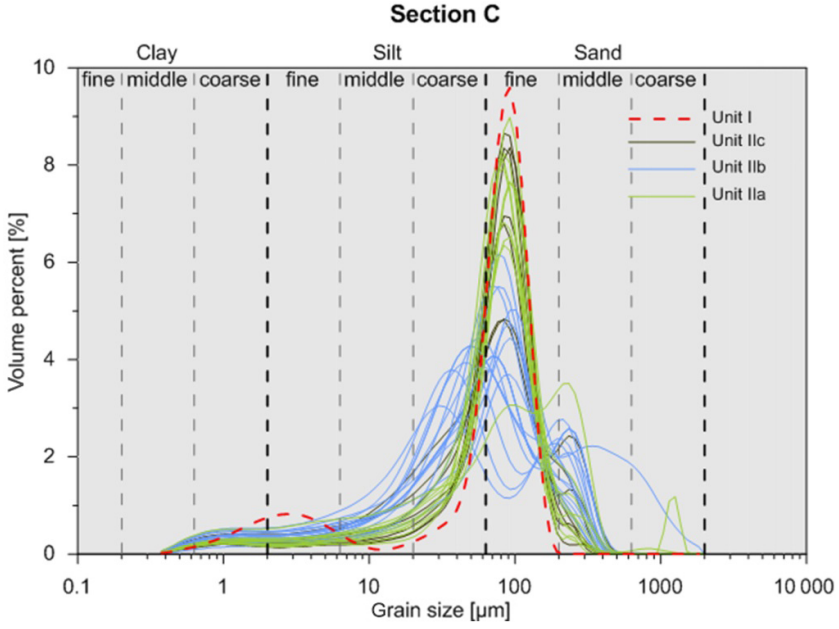

Figure 12. Grain size distribution plot for section C of the Batagay exposure.

Table 3. OSL and IRSL measurement data and respective dating results for the luminescence samples from Unit IV of the Batagay permafrost exposure Dose rate is the effective dose rate calculated based on results from gamma spectrometry and cosmic dose rate and corrected for mineral density, sediment density, grain sizes, and water content. Water is the in situ water content and saturation water content. *N* is the number of aliquots. PD is the palaeo-dose based on central age model, CAM, according to Galbraith et al. (1999). OD is the overdispersion. Age is the calculated ages according to CAM using the in situ water content. The > sign indicates that minimum age signals were close to saturation and hence tend to underestimate luminescence ages.

Sampling site	67°39′18″ N, 134°38′30″ E, 280 m a.s.l.							
Sample name	Depth [m]	Water [%]	Dose rate [Gy ka^{-1}]	Grain size [µm]	*N*	PD (CAM) [Gy]	OD [%]	Age [ka]
QUARTZ								
2.7/B/1/47	47	30.1/49.6	1.3	90–160	26	123.8 ± 6.2	26.5	> 93.6
			1.4	63–100	19	129.0 ± 6.1	17.1	> 95.2
2.7/B/2/47	47	34.3/51.6	1.3	90–160	11	127.1 ± 5.1	6.6	> 100.2
			1.3	63–100	11	185.3 ± 26.1	42.9	142.8 ± 25.3[a]
2.7/A/2/50	50	25.1/37.4	1.4	63–100	12	174.4 ± 14.4	23.7	> 123.2
FELDSPAR								
2.7/B/2/47	47	34.3/51.6		63–100	25	274.2 ± 3.32	3.9	210.0 ± 23.0[b]

[a] The CAM age using the saturation water content yields 160.9 ± 27.7 ka. [b] The age using the saturation water content yields 236.6 ± 24.0 ka.

overlying Units I–III. This sample is characterized by the largest sand fraction (70 %) and the highest carbonate content (8.2 wt %) of the studied sample set as well as the lowest MS value (13.7 SI).

OSL measurements for Unit IV in section B show that luminescence signals of quartz already reach the saturation level. For the two duplicate samples at 47 m b.g.s. (samples 2.7/B/1/47 and 2.7/B/2/47) and the one at 50 m b.g.s. (sample 2.7/A/2/50) only 11–26 out of 20–40 measured aliquots yielded equivalent doses and met the quality criteria of a recycling ratio within 10 % and a recuperation of below 5 %. Because of no significant skewness (below 1.5), age modelling was based on the central age model (CAM) according to Galbraith et al. (1999). However, the determined equivalent doses for several aliquots were still above the linear range of growth curves indicated by values above 2 times the D0 value and also by underestimation of applied doses during dose recovery tests. Hence, for the two measured grain sizes of the three samples, only minimum ages could be determined (see Table 3). Only for the sample 2.7/B/2/47 in the grain size 63–100 µm could an OSL age of 142.8 ± 25.3 ka be calculated. A note of caution concerns the water content. OSL ages were based on in situ water contents, for this sample 34.3 %, but samples were taken from unfrozen sediments, while the palaeo-water content of the frozen section remains unknown. To give an upper boundary condition, the saturation water content was used as well, and then the age of this sample yielded 160.9 ± 27.7 ka. Both age estimates lie at the common dating limits of OSL quartz techniques. For the same sample 2.7/B/2/47, feldspar was also available for luminescence dating. The feldspar grains of 63–100 µm showed bright IRSL signals and all 25 aliquots met the quality criteria. Equivalent doses that were determined were within the linear part of the growth curves and showed low errors and an extremely small data scatter, resulting in low overdispersion values of 3.9 % and no significant skewness (−0.32). The CAM yielded an IRSL age for feldspar grains of 210.0 ± 23.0 ka. If regarding the saturation water content as an upper boundary condition of the palaeo-water content, the IRSL age would increase by about 26 kyr (see Table 3 and respective notes).

According to the sedimentological characteristics of this material, Unit IV clearly differs from the overlying Units I–III. This sample is characterized by the largest sand fraction (70 %) and the highest carbonate content (8.2 wt %) of the studied sample set as well as the lowest MS value (13.7 SI).

4.6 Unit V

Unit V is exposed only at the deepest part of the thaw slump near the bottom of the profile (Fig. 6). The main part of this unit is not outcropping but buried. Even though only the truncated heads of ice wedges were exposed, the general composition of Unit V was easily observable and revealed ice-rich deposits in a layered cryostructure similar to the deposits of the YIC (Unit II), embedded in syngenetic ice wedges ≤ 4 m wide (Fig. 7g). Since Unit V exhibits distinct, separate ice wedges several metres wide beneath the layered Unit IV, it can be assumed to be a second ice complex older than the YIC. Unfortunately, Unit V was not accessible for sampling.

5 Discussion

5.1 Lithostratigraphy

According to field observations as well as geochronological and sedimentological data, the permafrost sequence of the Batagay mega-slump consists of five distinct stratigraphic units (Fig. 6a). No gradual transitions were observed between the units; thus, erosional events or strong changes of accumulation conditions can be expected to have occurred.

Unit I represents the active layer or, as we call it, the Holocene cover. The presence of a Holocene layer is typical of the majority of permafrost exposures, although it differs in thickness and age. For example, at Cape Mamontov Klyk it is 3 m thick and covers the time span from 9.5 to 2.2 ka (Schirrmeister et al., 2011b). The dating result from 1.15 m b.g.s. yielded an age of 0.295 ka, which suggests that much of the Holocene layer was eroded. The thickness is not constant along the Batagay outcrop and reaches a maximum observed depth of 1.4 m.

Unit II corresponds to the YIC. YIC deposits can form only under extremely cold winter conditions. They are thus indicative of cold stage climate in a continental setting. Our dating results confirm the assumption that the YIC was deposited from at least >51 to 12 ka BP, thus during the last cold stage and including the Marine Isotope Stage (MIS) 3 (Kargin) interstadial period. Huge syngenetic ice wedges and high segregation ice contents are the most typical features of YIC sequences. The structure of ice wedges intersecting sediment columns is evidence for the syngenetic freezing of the ice wedge polygon deposits. The ice wedges were 4.5 to 6.5 m wide, which indicates the impact of an extremely cold climate during their formation and also indicates aridity (Kudryavtseva, 1978). The thermokarst mounds (*baidzherakhs*) appearing in staggered order 4.5–6.5 m apart on the upper southeastern part of the YIC support this hypothesis.

The structural differences of the Unit II ice wedges suggest that they represent three generations of past ice wedge growth. Also, the threefold division of Unit II, as visible in its contour in the profile and in grain size parameters and TOC content in section C, may reflect three different climate stages, e.g. MIS 4, 3, and 2 during YIC formation. In this case, the MIS 4 and MIS 2 cold stadial phases were characterized by relatively uniform landscape conditions with fine sand accumulation and low bioproductivity, whereas the MIS 3 interstadial was characterized by changing accumulation conditions and higher bioproductivity. Unfortunately, the geochronological data do not support such subdivision since most dates are beyond the limit of the radiocarbon method. The coarse dating hence does not imply continuous sedimentation during the last 51 kyr; thus, we cannot exclude interruptions in the sedimentation record. Also, we could not take samples directly from the visually different subunits in the western part near section A (Fig. 6d) to verify if sedimentological characteristics confirm the apparent visual differences. The YIC at parts of section A differed from the YIC in other parts of the exposure in having considerably smaller outcropping ice wedges. We considered the absence of visible large ice wedges due to exposed intra-polygonal sediment sequences concealing the ice wedges at this place. Owing to the lack of large exposed ice wedges, this part of the sequence was, however, separated from the YIC and regarded as its own unit by Murton et al. (2016).

Dating results may indicate that parts of the YIC could have been eroded. Taken at a depth of 2.05 m b.g.s., the uppermost dated sample of Unit II in section A has an age of ca. 33 ka BP. The dating of the next overlying sample with a position in Unit I only about 1 m above resulted in an age of ca. 0.3 ka BP. This young age might be the result of contamination with modern material. No features of cryoturbation were observed but the horizon included roots of modern plants. Cryoturbation is very unlikely since the ground is not wet enough for cryoturbation due to inclination and fast drainage. No Holocene sediments older than the 0.3 ka BP sample at 1.15 m b.g.s. in section A have yet been found in the Batagay mega-slump, but this could be due to the difficulty of accessing the upper parts of the profile. The youngest YIC age in section A of about 26.2 ka BP originates from plant material amassed in a ground squirrel nest 4.6 m b.g.s. The age inversion between 2.05 and 4.6 m might be the result of younger material actively transported by arctic ground squirrels deep into their subterranean burrows for food storage. Together with the fault tolerance of the radiocarbon dating, this might explain the inversion. The assumption of plant material transport by ground squirrels is reasonable for depths of up to 1 m below ground, which is an average depth for the permafrost table. The permafrost table as a natural barrier for ground squirrel penetration can be even deeper, when the soil substrate is coarse-grained and dry as is often the case for sandy deposits. Larionov (1943) reported on a ground squirrel nest found in Siberia at 2 m depth.

Due to the uncertainty of the age–height relation, we redated material from the ground squirrel nest and obtained an age of about 25 ka BP, which confirms the original dating (Table 2). The substrate at the site is sandy and, during the lifetime of the ground squirrel, it was probably dry due to the inclination at this slope. The eventuality that the overlying older age originates from redeposited material from further uphill must however be taken into account as well.

The youngest YIC age from the Batagay thaw slump of about 12.7 ka BP was determined in section C (southeastern part) at 8.5 m b.g.s. This result stresses the difference between southeastern and northwestern parts of the outcrop. An age gap of several tens of thousands of years could be expected between the infinite age of >48 ka BP at 12.5 m b.g.s. and 12.7 ka at 8.5 m in section C. It is implausible that only 4 m of YIC deposits were formed during more than 35 kyr.

The observed stratigraphic hiatus of up to 12 kyr atop the YIC was likely caused by post-depositional erosional events, such as widespread thermo-denudation or local thermal ero-

sion of early Holocene deposits. A sudden shift from deposition to erosion as a consequence of intense warming during the late glacial–early Holocene transition (e.g. Bølling–Allerød) and also during other warm phases such as the middle Weichselian interstadial is a characteristic feature of many YIC sequences in Yakutia (e.g. Fradkina et al., 2005; Wetterich et al., 2014; Schirrmeister et al., 2011b) and can also be readily assumed for the Batagay thaw slump. The uppermost boundary of YIC sequences as dated with the AMS radiocarbon method differs between 28 ka BP on the New Siberian Islands and 17–13 ka BP at various other sites. Available radiocarbon dates from mature *alas* depressions in central Yakutia reported to have an age of 12 ka BP (Katasonov et al., 1979; Kostyukevich, 1993).

The organic layer of Unit III below the base of the YIC (Unit II) is characterized by a high abundance of macroscopic plant material including woody remains. Plant macrofossil analyses reveal taxa characteristic of northern taiga forests with larch (*Larix gmelinii*), birch (*Betula* spp.), shrub alder (*Alnus fruticosa*), and indicators of dry and open habitats (Ashastina et al., 2015). The palaeobotanical results clearly indicate warm climate conditions during the formation of this layer. High values of TOC and C / N and low δ^{13}C values reflecting increased bioproductivity and moderate organic-matter decomposition confirm this suggestion. These proxy records together with the position of Unit III below the base of the YIC, the infinite AMS date of > 44 ka BP of the sample, and the OSL quartz date of 142.8 ± 25.3 ka of the sample taken from Unit IV indicate that Unit III probably formed during the MIS 5e interglacial. This assumption is in good agreement with data from Lake El'gygytgyn (Tarasov et al., 2013), where the Eemian interglacial from 127 to 123 ka was the warmest period in the last 200 kyr. The organic layer of the Batagay Unit III is continuous throughout the outcrop and shows a uniform thickness of about 1.5 m, reaching up to 3.5 m in thickness in palaeo-depressions. Such a distribution might indicate the presence of a continuous palaeosol that developed under stable interglacial conditions.

The uniformly occurring Unit IV with its characteristic horizontal bedding was observed over large distances along the lower and very steep segment of the exposure wall. The lack of wide ice wedges or ice wedge casts indicates that the conditions during deposition of Unit IV were inappropriate for the formation of a pronounced ice complex directly below the last interglacial Unit III. Unit IV instead represents sediments that, in contrast to YIC deposits, consistently accumulated under uniform depositional environments. We did not find any evidence for the presence of lacustrine or fluvial deposition in the sediments along the whole permafrost sequence. We detected neither pebbles, other coarse material, nor freshwater mollusc remains. Fluvial or lacustrine deposition can be excluded because of the topographical setting: the area around the Batagay mega-slump is northeastwardly inclined. This would prevent water stagnation and would not result in clear horizontally layered structures. Instead, laminar slope deposition as the result of ablation or aeolian activity can be assumed to be the main sedimentation processes that formed Unit IV. The assumed laminar slope deposition can be related to cryoplanation and other nivation processes during cold phases, with perennial snow accumulations further uphill. Detailed sedimentological results are not available for Unit IV since it was not accessible for sampling during our field stay. A detailed description of this unit was presented by Murton et al. (2016).

The lowermost Unit V was observed in the field at the bottom part of the thaw slump wall (Figs. 6, 7g). The existence of truncated ice wedges several metres in width and their position more than 20 m below Unit III, which represents the last interglacial period, allow the interpretation that this unit represents an ice complex indicating a continental cold-stage climate with extremely cold winters already occurring during the Middle Pleistocene. The symmetric ice wedges contained in the unit point to the syngenetic formation of Unit V. The finding of such ancient ice wedges also demonstrates that ice-rich permafrost survived at least two glacial–interglacial cycles (MIS 5 and MIS 1). Similar observations of ice complex deposits older than the last interglacial were made on Bol'shoy Lyakhovsky Island by Andreev et al. (2004) and Tumskoy (2012) and were dated by Schirrmeister et al. (2002) to MIS 7. On the basis of the stratigraphical position of this ice complex below Unit III, which is thought to be deposited during the last interglacial, we assume that Unit V is older than MIS 5e, thus of the Middle Pleistocene age.

An overview of changes in palaeoclimatic conditions and the response to these changes reflected in the sediment sequence of the Batagay mega-thaw slump is available in Table 4. The shifts in sedimentation characteristics of the Batagay sequence are in good agreement with global climatic events, such as glacial and interglacial phases recorded by oxygen isotope data, and regional climatic changes, identified by stadial–interstadial phases in Siberia and Europe.

5.2 Sedimentation processes of the Batagay YIC

Our reconstruction of YIC formation is based on the analysis of GSD as discussed in Sect. 4. Additional studies on the mineralogical composition as well as micromorphological analysis would be useful to identify the sources more precisely. The radiocarbon dating results of the YIC in the Batagay mega-slump from > 51 to 12 ka BP with large gaps in between suggest that the sedimentation experienced interruptions or parts of the sequence were eroded. In addition to post-depositional erosion, the gaps within Unit II might also be the result of temporarily and spatially shifted local deposition. Sediments were deposited during given periods and at a particular part of today's outcrop mainly from a certain source area, such as Mt. Kirgillyakh northeast of the outcrop; during earlier or later periods, sedimentation might have stopped there and instead taken place mainly at another

Table 4. Overview of permafrost dynamics recorded in the Batagay sequence in presumable correlation with global and regional climate histories. Due to the sparse dating resolution, the correlation is mainly based on the chronostratigraphic comparison of Batagay and lowland exposures. Global climate history is represented by marine isotope stages (MISs; Aitken and Stokes, 1997) derived from the δ^{18}O curve (modified from Pisias et al., 1984), reflecting global temperature changes studied in deep sea cores. Negative δ^{18}O ‰ values reflect warm climate stages, while positive values identify cold phases. The regional Siberian climate phases are given according to Sachs (1953). The European regional climate events for comparison are named according to Litt et al. (2007).

δ^{18}O (‰) 2 1 0 -1 -2	Date BP, ka	MIS	Siberian classification	European classification	Unit	Permafrost dynamics
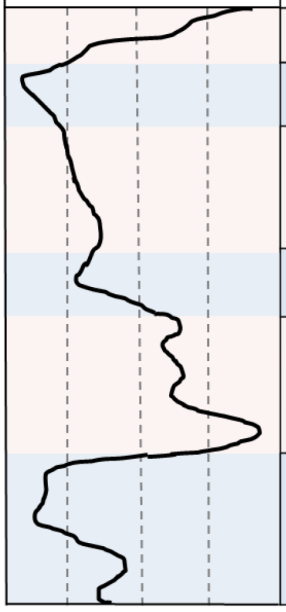	< 11.5	1	Holocene	Holocene	I	Permafrost degradation, erosional processes
	28 – 11.5	2	Sartan stadial	Late Weichselian	IIc	Yedoma Ice Complex, thickest ice wedges - coldest climatic conditions
	50 - 28	3	Kargin interstadial	Middle Weichselian	IIb	Yedoma Ice Complex with warm phase signals – TOC values higher than in Unit IIc and IIa
	73 - 54	4	Zyryan stadial	Early Weichselian	IIa	Yedoma Ice Complex agradation – thick ice wedges, low organic content
	120 - 127	5	Kazantsevo interglacial	Eemian	III	Thick organic layer, warmest period within the sequence
	> 130	6	Taz stadial	Late Saalian	IV	Cessation of ice complex formation, increased sedimentation rates, shift in climatic conditions
				?	V	Middle Pleistocene Ice Complex, thick ice wedges, cold stage climate

part of the foothill and from a different local source area, e.g. Mt. Khatyngnakh southwest of the outcrop (Fig. 1c). Due to varying discharge directions, locally restricted denudation phases might also have occurred. As a result, the entire YIC sequence might not have formed simultaneously, but may have formed piecewise and successively.

We assume that the sediment material was subaerially exposed and was incorporated into the permafrost syngenetically, e.g. at the same time as the deposition. The final accumulation occurred within small depressions of low-centre polygons, which existed between the ice wedges. The exposed YIC wall is a cross section through the former landscape with polygonal patterned ground.

According to the general scheme of landscape types introduced in Schirrmeister et al. (2011b), the Batagay YIC is related to the second landscape type, which represents cryoplanation terraces occurring on foothill slopes. The first landscape type is low-elevation coastal mountains and foreland accumulation plains; the third landscape type is extended lowland at a great distance from mountain ranges. After 60 ka BP, local mountain glaciers no longer reached the highlands (as was true during the Middle Pleistocene), but glaciation covered only the western and southwestern Verkhoyansky Mountains (Siegert et al., 2007). Hence, the bedrock in the study area could have been affected by strong frost weathering providing fine-grained material for aeolian transport and YIC formation. Such bedrock weathering is also typical of the permafrost sequences at Bol'shoy Lyakhovsky Island, Cape Svyatoy Nos, and the Stolbovoy and Kotel'ny islands (Siegert et al., 2009).

A possible sediment supplier is located 20 km south of the Batagay thaw slump: Mat' Gora, a 1622 m high massif (Fig. 1b). We suggest however that Mt. Kirgillyakh and Mt. Khatyngnakh, situated just 2 km away (Fig. 1c), mainly provided substantial input to the sediment composition of the Batagay deposits. YIC subunit IIa and IIc are characterized by a unimodal distribution curve made up by a > 50 % fine-grained sand fraction; this can be explained as a result of periglacial, proluvial, or nival processes (Kunitsky et al., 2002). We suggest that subunit IIc correlates to the MIS 2 (Sartan) stadial and subunit IIa correlates to the MIS 4 (Zyryan) stadial.

According to Kunitskiy et al. (2013), nival processes were highly significant here during the late Pleistocene. They proposed that nival (snow-filled) depressions existed at this time; thus, cryohydro-weathering, as discussed by Konishchev (1981), took place. The material trapped on top of

the snow was, during snow melt, incorporated into downslope sediments.

In addition to the nival genesis of the sediments, the material trapped by snow could have been transported there by local aeolian processes, as the coarse-silt fraction of 30–50 µm suggests. Some horizons are characterized by less than 40 % of silt in the GSD, thus indicating that aeolian input, although it is significant, might not have been the main and only deposition process. The Batagay mega-slump is located within 10 km of the Yana River and 30 km from the Adycha River floodplains. The meandering pattern of both river systems and the adjacent sandy terraces ≤ 50 m high (Fig. 1c, upper left) suggest that, during the Late Pleistocene, when the continentality and wind velocities were higher than today, the wide, braided floodplains could have provided material for local aeolian input. Local aeolian input could originate from the Batagay river floodplain as well (Murton et al., 2016). Even though the substrate is stabilized almost everywhere by vegetation, today the sandy terraces of the Yana River also provide large amounts of material available for local dust storms in summer. The results of MS measurements did not display, however, any changes in the content of magnetic or magnetizable minerals within the studied sequence as would be expected from shifts in the main source areas, e.g. from local slope deposits to more regional, redeposited alluvial material from the Yana River.

The GSD curves for Units IIb and III indicate a polygenetic sediment origin; this is indicated by the bimodal distribution in fraction sizes, from silt and coarse silt – a possible aeolian transport indicator – to sand, a possible hint of proluvial and nival genesis, as was discussed for subunit IIa and IIc. Nevertheless, the high percentage of the silt fraction in the GSD of subunit IIb cannot be interpreted as an exclusive indicator of aeolian deposition because high silt content in the sediment composition can also result from cryogenic disintegration of quartz due to repeated thawing and freezing cycles (Konishchev and Rogov, 1993; Schwamborn et al., 2012). The predominance of silt in the GSD might be a result of the combination of both processes, frost weathering and aeolian deposition.

However, the Batagay source material certainly differs from that in the coastal outcrops. Bykovsky was fed by the Khara-Ulakh Mountains, a low-elevation coastal mountain ridge. In contrast, Batagay was supplied with sediments from the hillside of the Kirgillyakh–Khatyngnakh eminence. Another possible material source for Batagay is windblown material from the Yana River valley and Adycha River valley; this is suggested by the occurrence of sandy terraces adjacent to the Yana floodplain 7 km west of the Batagay outcrop (Fig. 1c, upper left part).

A certain proportion of local aeolian deposition in the formation of the Batagay YIC is indicated by its sedimentological characteristics. Despite similarities in the general YIC (Unit II) structure, the Batagay sequence is distinct from other permafrost exposures. All coastal outcrops are characterized by polymodal grain size curves, a dominance of fine-grained sediments, and relatively high concentrations of silt in their structure. The Batagay YIC, in contrast, is dominated by fine-grained sand in a unimodal GSD curve (Unit IIa and c) and by bimodal coarse-silt and fine-sand curves (Unit IIb). Higher concentrations of sand in the YIC exposures of Kurungnakh Island and Diring Yuriakh (Lena River delta) are interpreted to be of aeolian origin (Siegert et al., 2009; Waters et al., 1997).

The characteristics of the Batagay YIC profile could be assumed to be close to the Mus-Khaya or Mamontova Gora outcrops because the first is located along the Yana River bank and is in a comparable hydrological location, while the second, from the Aldan River in Central Yakutia, is another example of an inland YIC that never experienced maritime influence. Although also situated in the catchment area of the Yana–Adycha river system, the Mus-Khaya ice complex (Katasonov, 1954) is hardly comparable to the Batagay YIC. In contrast to Batagay, the Mus-Khaya ice complex is affected by fluvial deposition resulting in a cyclic facial-lithological structure represented by dark-brown, organic-rich, loess-like loam alternating with dark-grey, ice-rich loam. This alternation of organic-rich and ice-rich sediments of different composition is the basis of the cyclic YIC structure theory because the deposits are believed to be of predominantly alluvial origin (Katasonov, 1954; Lavrushin, 1963; Popov, 1967). This theory can be well implemented for floodplain settings because the cycles represent changes governed by shifts in the river course, from riverbed to oxbow lake and floodplain deposits. Such cyclic structure is not detectable at the Batagay outcrop because this site was not affected by river influence as it is distant from a river floodplain. On the contrary, the absence of such cyclic structure indicates the slope genesis of the studied YIC.

Seasonally controlled processes under the influence of a continental climate might have governed the deposition of Unit II; during the cold winter, nival deposition could have been dominant, whereas proluvial and aeolian deposition could have prevailed during the snowmelt period and the dry summer season. Aeolian deposition was thus locally restricted and was one of several processes that formed the Batagay ice complex sequence.

5.3 Climatic implications in comparison with other ice complex sequences (inland versus coastal ice complex)

The Batagay mega-slump studied here shows a general structure comparable to coastal permafrost exposures of Quaternary deposits in northeastern Siberia, as described by Schirrmeister (2011a), as follows: (i) late Saalian ice-rich deposits (ancient ice complex), (ii) pre-Eemian floodplain deposits, (iii) Eemian thermokarst deposits, (iv) alluvial deposits from the Eemian–Weichselian transition, (v) early,

middle, and late Weichselian ice-rich deposits (YIC), and (vi) late glacial and Holocene thermokarst deposits.

Using the abovementioned general structure of permafrost sequences in the coastal lowlands, we subsequently compare the Batagay units with other Quaternary sediment records in northeastern Siberia.

The Holocene unit at the Batagay outcrop is represented by a thin cover of up to 1.4 m. The only available date reveals an age of 300 years BP. Further dating along the upper edge of the exposure is necessary for the differentiation of late glacial and Holocene deposits. During the late glacial and the Holocene, the YIC and more recent sediments were often eroded due to climatic warming. Thermo-erosion of the upper YIC layer is typical for most of the known permafrost exposures. For example, thermokarst depressions filled with organic deposits are observed at Cape Mamontov Klyk. At the New Siberian Archipelago, the Holocene cover is still partly present (Schirrmeister et al., 2011b).

The YIC, corresponding to Unit II in the Batagay profile, is the most-accessible and best-studied Quaternary permafrost sediment type in Siberia. The YIC developed during MIS 4–MIS 2. Kaplina (1981) estimated the MAGT during YIC aggradation on the basis of such parameters as the width of ice wedges, typical polygon sizes, the temperature coefficient of rock contraction, and values of −20 to −25 °C obtained for the late Pleistocene (today −7.7 °C). Similar values can be assumed for the time of formation of the Middle Pleistocene ice complex – Unit V in the Batagay profile. Ice complex characteristics such as spacing and width of ice wedges cannot reliably be used to estimate mean annual air or even mean winter palaeotemperatures (Kaplina, 1981; Plug and Werner, 2008). However, Romanovskii et al. (2000b) indicated a MAGT 8 °C lower than today during MIS 4 and MIS 3 and 10 °C lower than today during MIS 2 for the coastal lowlands. Siegert et al. (2009) summarized the results of the Russian–German decadal cooperation on the investigation of coastal YIC in northeastern Russia with special attention to sites at Cape Mamotov Klyk, the Lena Delta, Bykovsky Peninsula, Bol'shoy Lyakhovsky Island, and the northern islands of the New Siberian Archipelago. According to the dating results, coastal ice complexes were preserved until 27 ka BP at the New Siberian Archipelago, while along the mainland Laptev Sea coast, younger deposits are also available. Konishchev (2013) suggested a YIC formation time frame from 50 to 11 ka BP. The youngest dates of Batagay YIC deposits have an age of 12 ka BP. The cessation of YIC formation might explain the hiatus in the sedimentation record from 12 to 0.3 ka BP in the Batagay sequence. Such gaps, even though not of such magnitude, also exist in exposures at Kurungnakh Island, the Lena Delta (Wetterich et al., 2008), Molotkovsky Kamen, and Malyj Anjuy River (Tomirdiaro and Chernenky, 1987). Gaps in sediment preservation might also be explained by locally increased erosion triggered by changes in climatic conditions. According to Kaplina (1981), sedimentation gaps are possibly connected to large-scale thermokarst processes as well as an increase in humidity and forest cover. The moister Holocene climate of this area was governed by changes in the hydrological regime, which was triggered by the transgression of the Laptev and East Siberian seas. Peatland deposits as indicators for thermokarst processes as they are characteristic for early Holocene sites in the circum-Arctic (MacDonald et al., 2006) were not detected at the Batagay outcrop. This might be due to the absence of intense thermal degradation or due to the topographical setting preventing meltwater from accumulating. In the Batagay profile, we detected neither lacustrine nor palustrine deposits, which might be indication of thermokarst processes.

Based on detailed studies of YIC in Siberia, Katasonov (1954) detected a cyclic structure of sediments in the Mus-Khaya outcrop. This concept was further developed by Lavrushin (1963) and Romanovskii (1993) and summarized by Konishchev (2013). The identified lithogenetic cycles depict changes in climate conditions that occurred from MIS 4 to MIS 2, e.g. two stadial stages (Zyryan and Sartan) and one interstadial stage (Kargin) with several thermochrones within. On the basis of sedimentological and TOC analyses, we also distinguished three subhorizons in the YIC structure (subunit IIa to IIc). Konishchev (2013) described such cyclic sediment cryostructures as consisting of alternating layers of heavily deformed greenish-grey ice-rich loam, peat inclusions, less ice-rich non-deformed strata, and brown loam with a fine layered cryostructure. Such sedimentation cycles, governed by a floodplain setting, are mentioned, e.g. for the Mus-Khaya, Duvanny Yar, and Chukochiy Yar outcrops (Kondratjeva, 1974; Kaplina et al., 1978; Konishchev, 2013). In Batagay, such cyclicity could not be detected partly due to the specific cross section of the steep southwestern permafrost wall (this wall was mostly cut along the wide ice wedges), partly owing to the lack of accessibility of the unit II along the whole exposure. However, at the more gentle southeastern part of the outcrop, such structures also did not occur, possibly due to a different geomorphological setting as discussed below.

The subdivision of the Batagay YIC is similar to that of Mamontovy Khayata at the Bykovsky Peninsula (Schirrmeister et al., 2011b). Accordingly, the middle parts of both YIC sequences contain MIS 3 peat horizons, indicating warm phases. In Unit IIb of the Batagay sequence, two horizons rich in organic carbon were identified (Fig. 12). The upper part of Mamontovy Khayata is composed of proluvial MIS 2 (Sartan) deposits resembling Unit IIa in Batagay.

Mamontova Gora is situated along the Aldan River in central Yakutia, outcropping in a 50 m high terrace (Markov, 1973). It was stratigraphically subdivided into three units covering the time span from the Holocene to presumably the last interglacial (Péwé et. al., 1977). The middle unit of the Aldan River outcrop revealed radiocarbon ages from 26 ka BP to > 56 ka BP, which correlate to Unit II in the Batagay sequence and supports the assumption that an erosional

event took place in central Yakutia on a similar temporal scale as in the Yana Highlands. The Mamontova Gora sequence in contrast to the Batagay profile is composed of 60 % of well-sorted silt with grain size values of 0.005–0.5 mm, which was explained by distant aeolian particle transport from wide, braided, unvegetated flood plains of rivers draining nearby glaciers (Péwé et. al., 1977).

Most of the coastal permafrost exposures in Siberia are characterized by bimodal or polymodal GSD curves (Schirrmeister et al., 2008, 2011b), which indicate a variety of transport, accumulation, and resedimentation processes occurring there. Unimodal and bimodal curves, as were revealed for both Mamontova Gora and the Batagay megathaw slump, could reflect more stable accumulation and sedimentation processes under continental conditions.

Unit III in the Batagay outcrop might be equivalent to part III of the general permafrost sequence structure (i.e. MIS 5e) with a few differences. Its structure is referred to as a lake thermokarst complex (Tomirdiaro, 1982) or as ancient Achchagyisky and Krest Yuryakhsky *alas* deposits (Kaplina, 2011) and is displayed in peat layers ≤ 10 m thick filling former ground depressions, e.g. ice wedge casts. This horizon formed as a result of permafrost thaw processes during the last interglacial (MIS 5e) warming and is present with variable thicknesses in all permafrost exposures from the coastal zone, e.g. from Duvanny Yar, the Kolyma River (Kaplina et al., 1978) and Mus-Khaya, and the Yana River (Katasonov, 1954; Kondratjeva, 1974) to exposures further inland, e.g. the Allaikha and Sypnoy Yar outcrops, the Indigirka River (Lavrushin, 1962; Kaplina and Sher, 1977; Tomirdiaro et al., 1983), Mamontova Gora, and the Aldan River (Péwé et al., 1977). The peat horizon can occur continuously or only in scattered peat lenses as is the case in the Allaikha profile. At the Batagay profile, we noticed a rather thin (about 1 m thick) layer with pronounced lenses ≤ 5 m thick filling former ground depressions. Gubin (1999) and Zanina (2006) studied the palaeosols of the ancient *alas* complex at Duvanny Yar and suggested that two types of soil occurred there: peat bog soils and peaty floodplain soils, both indicating wet ground conditions. Preliminary palaeobotanical analyses of Unit III deposits at the Batagay profile revealed exclusively terrestrial plant remains, no aquatic or wetland plants. Our data accordingly suggest that northern taiga with dry open-ground vegetation existed at Batagay during the MIS 5e interglacial (Ashastina et al., 2015). The presence of larch, birch, and alder in the species composition suggest that climatic features, such as temperature, precipitation, and snow cover thickness, were suitable for forest establishment in the continental part of inland Siberia during the Eemian. The tree species in light taiga forests require a mean temperature of the warmest month of at least 12 °C (Andreev, 1980). Coarse woody fossils are absent at Bol'shoy Lyakhovsky Island (Wetterich et al., 2009) and are sparsely present in records from coastal permafrost exposures, e.g. Oyogos Yar, and Allaikha River exposures (Kaplina et al., 1980; Kienast et al., 2011). The pronounced continentality in Batagay provided suitable climatic conditions for a forest development more intense than in coastal settings during the Eemian. Dry ground conditions with limited peat accumulation during the formation of Unit III might also be due to the relatively low ice content of the underlying Unit IV, which, when the MIS 5e warming started, resulted in less available meltwater from thawing permafrost.

Pre-Eemian deposits (as described for part II of the general classification) were detected on Bol'shoy Lyakhovsky Island (Schirrmeister et al., 2011b) and Oyogos Yar (Kienast et al., 2011). The position of Unit IV in the Batagay outcrop stratigraphically matches the abovementioned pre-Eemian floodplain deposits in the general classification of coastal permafrost exposures from Schirrmeister et al. (2011a). Unfortunately, we could not sample and analyse enough material from Unit IV to reconstruct its genesis, but according to our field observations (appearance and structure of the unit), it is unlikely that the material is of subaquatic origin. The main reason for the absence of temporary and permanent water bodies at the site might be the relief gradient and associated rapid drainage of surplus waters after snowmelt and permafrost thawing. In this setting, intensified rates of frost weathering of the surrounding mountains' bedrocks and increased slope deposition of alluvial material are regarded as the main deposition sources. Ice wedges as prevailing in the underlying Unit V or ice wedge casts are absent in Unit IV. The abrupt transition between both strata suggests a cessation of ice complex formation owing to a sudden climate shift. We assume that ice wedge growth ceased because of boosted sedimentation disrupting frost cracks. Also, milder winter temperatures and/or higher snow accumulation preventing thermal contraction and frost cracking are conceivable.

Unit V of the Batagay outcrop is represented by the truncated heads of wide ice wedges indicating ice complex deposits older than the MIS 5e. Similar structures with a comparable stratigraphic position, corresponding to part I of the general structure of coastal permafrost exposures, were observed on Bol'shoy Lyakhovsky Island and dated back to 200 ka BP (Schirrmeister et al., 2002; Andreev et al., 2004; Tumskoy, 2012). Ice complex is syngenetically frozen sediment containing a grid-like system of large ice wedges resulting in a ground surface pattern of polygonal ridges encircling small depressions, which during ice complex genesis, act as sediment traps. Polygonal ice wedges form due to repeated thermal contraction of the frozen ground, resulting in netlike arranged cracks that are filled in the spring by snow meltwater, which immediately freezes and forms ice veins. A mean annual air temperature lower than -8 °C is regarded as the threshold for ice complex formation (Plug and Werner, 2008). Polygonal ice wedge systems are indicative for continental cold stage climate with very cold winter air temperatures and annual ground temperatures. Ice wedge growth is not only influenced by climate but also by local factors

such as ice content, grain size distribution, vegetation, and snow depth. However, ice complex deposits clearly indicate climate conditions much colder than present.

The Batagay outcrop is one of the few permafrost profiles accessible in interior Yakutia. The present study offers rare insights into the evolution of northern environments under the conditions of the most severe climatic continentality in the Northern Hemisphere. We suppose that differences in continentality between inland and coastal sites were more crucial during warm intervals, when sea levels were high and coastlines shifted southward. This is supported by the presence of forest plant taxa in the inland exposure (Batagay) and their absence in coastal lowlands (e.g. New Siberian Islands) during the Eemian interglacial. The influence of continentality is greater than the effect of latitude as can be observed by the southward shift of the tree line in coastal areas of Chukotka and Alaska with a more oceanic climate. Summer temperature is more crucial for the vegetation than winter or mean annual temperature. More detailed climate reconstructions should be conducted for the Batagay site using palaeoecological methods in order to test this assumption in the future. Further studies should also be focused on cryolithological analyses of material from Units IV and V to fill the current gaps in knowledge about the formation of these units. Furthermore, studies on ice wedge stable isotope composition will provide valuable information on past winter climate (e.g. Meyer et al., 2002, 2015) necessary for the reconstruction of the palaeoclimatic seasonality at the highly continental site of Batagay. Sedimentological, cryolithological, and stable isotope analyses and the study of fossil bioindicators (plant macrofossils, pollen, insects, and mammal bones) will contribute to the reconstruction of Quaternary palaeoenvironments in western Beringia.

6 Conclusions

- The Batagay mega-thaw slump is one of the few active permafrost outcrops in interior Yakutia, which provides rare insights into sedimentation processes and climate and environmental evolution under the conditions of the most severe climatic continentality in the Northern Hemisphere.

- As indicated by OSL dates, the exposed sequence has been deposited over a large time span, at least since the Middle Pleistocene.

- Altogether, five distinct sedimentological units, representing different accumulation phases, were detected (top to bottom): a Holocene cover layer; the Late Pleistocene YIC; an organic horizon deposited during the last interglacial; a thick, banded, uniform unit without visible ice wedges; and another ice complex older than the last interglacial.

- The detected five cryolithological units reveal distinct phases in the climate history of interior Yakutia: the existence of a Middle Pleistocene ice complex indicates cold stage climate conditions at the time of deposition of Unit V resulting in a MAGT at least 8 °C lower than today.

- A climate shift during deposition of Unit IV caused cessation of ice wedge growth due to highly increased sedimentation rates and eventually a rise in temperature.

- Full interglacial climate conditions existed during accumulation of the organic-rich Unit III. In contrast to other MIS 5e deposits in Yakutia, e.g. in the coastal lowlands, no plant or mollusc remains indicating aquatic or palustrine environments could be detected. On the contrary, plant macrofossils reflected open forest vegetation existing under dry conditions during the last interglacial.

- The late Pleistocene YIC (MIS 4–MIS 2) occurring in Unit II proves the presence of severe cold-stage climate conditions with a MAGT 8 to 10 °C lower than today.

- Peatland deposits as indicators for thermokarst processes, as they are characteristic for early Holocene sites in the circum-Arctic, were not detected at the Batagay outcrop. This might be due to the absence of intense thermal degradation or due to the topographical setting preventing meltwater from accumulating.

- As is indicated by radiocarbon AMS dating, gaps in the sedimentological record likely exist as a result of erosional events or of spatially and temporarily differential small-scale deposition.

- Compared to other YIC sites in Yakutia, Unit II of the Batagay profile could be classified as a highland type of YIC, which is characterized by its geographical position distant from rivers and sea coasts and in proximity to hills and mountains more inland. Whereas fluvial and lacustrine influence is common for certain depositional periods in the majority of permafrost exposures on the Yakutian coastal lowlands, it has to be excluded for the Batagay sequence.

- We suggest that the prevailing sedimentation processes and the sources for the deposited material varied seasonally during the formation of the YIC in the Batagay profile.

Data availability. The sedimentological data sets and the age determination (OSL method) runs of the samples reported in this paper were uploaded to PANGEA (https://doi.pangaea.de/; Ashastina et al., 2017).

Author contributions. FK designed the study conception and arranged the expedition. FK and KA carried out field description and sampling. LS accomplished the sedimentological analysis and plotted the graphs. MF designed and performed the OSL dating procedure and interpretation. KA, LS, FK, and MF participated in drafting the article. KA and FK prepared the paper with contributions from all co-authors. FK, LS, and KA revised the draft.

Competing interests. The authors declare that they have no conflict of interest.

Acknowledgements. This research was funded by the German Science Foundation (DFG, KI 849/4-1) and supported by the German Federal Ministry of Education and Research (BMBF, Arc-EcoNet, 01DJ14003). We sincerely thank Elena Troeva from the Institute for Biological Problems of the Cryolithozone Yakutsk, who provided great support in coordination, planning, and in logistical processes. We thank our Russian colleagues for great support during fieldwork in Batagay, especially for the patience and never-ending help in transport by Vladimir Malyshenko, and for the hospitality of Anna Jumshanova and Sargylana Sedalischeva and their willingness to organize a small home lab. Thanks to the team of Ludmila Pestryakova from the North-Eastern Federal University Yakutsk for help with the sample logistics. We gratefully acknowledge prompt work on dating under the supervision of Tomasz Goslar at the Poznan Radiocarbon Laboratory, Poland. The analytical work in AWI laboratories was expertly conducted by Dyke Scheidemann. We are grateful for the helpful and constructive comments on the paper by Christine Siegert and Sebastian Wetterich from the Alfred Wegener Institute, Helmholtz Centre for Polar and Marine Research Potsdam, and Thomas Opel from the University of Sussex, UK. We thank Benjamin Gaglioti, Duane G. Froese, and the anonymous reviewer for critical comments and valuable suggestions.

Edited by: Denis-Didier Rousseau
Reviewed by: Duane G. Froese, Benjamin Gaglioti, and one anonymous referee

References

Aitken, M. J. and Stokes, S.: Climatostratigraphy, in: Chronometric dating in archaeology, edited by: Taylor, R. E. T. and Aitken, M. J., chap. 1, Springer Science & Business Media, New York, USA, 1–30, 1997.

Andreev, A. A., Grosse, G., Schirrmeister, L., Kuzmina, S. A., Novenko, E. Y., Bobrov, A. A., Tarasov, P. E., Ilyashuk, B. P., Kuznetsova, T. V., Krbetschek, M., and Meyer, H.: Late Saalian and Eemian palaeoenvironmental history of the Bol'shoy Lyakhovsky Island (Laptev Sea region, Arctic Siberia), Boreas, 33, 319–348, 2004.

Andreev, V. N.: Vegetation and Soils of Subarctic Tundra. Academy of science, Siberian Subbrunch Biological Institute, Nauka, Novosibirsk, Russia, 1980.

Ashastina, K., Reinecke, J., Wesche, K., and Kienast, F.: A newly formed permafrost outcrop in Batagay, Arctic Siberia sheds light on the Eemian vegetation of Beringia, 1st Central European Polar Meeting, 10–13 November 2015, Vienna, Austria, 2015.

Ashastina, K., Schirrmeister, L., Fuchs, M. C., and Kienast, F.: OSL age determination and sedimentological characteristics of the Batagay thaw slump, Northeastern Siberia, https://doi.org/10.1594/PANGAEA.877346, 2017.

Astakhov, V.: The postglacial Pleistocene of the northern Russian mainland, Quaternary Sci. Rev., 92, 388–408, https://doi.org/10.1016/j.quascirev.2014.03.009, 2014.

Baranova, Yu. P.: Neogene and Pleistocene deposits of Central Yakutia, Guidebook XIV Pacific Science Congress, Yakutsk, 12–18 August 1979, Yakutsk, Russia, 37–73, 1979.

Bøtter-Jensen, L., Andersen, C. E., Duller, G. A. T., and Murray, A.S.: Developments in radiation, stimulation and observation facilities in luminescence measurements, Radiat. Meas., 37, 535–541, 2003.

Bronk Ramsey, C.: Bayesian analysis of radiocarbon dates, Radiocarbon, 51, 337–360, 2009.

Carter, M. R. and Gregorich, E. G. (Eds.): Soil Sampling and Methods of Analysis, second ed., Taylor and Francis, London, UK, 1224 pp., 2007.

Duller, G. A. T.: Analyst v4.31.7 user manual, Aberystwyth Luminescence Research Laboratory, Technical report, Aberystwyth University, Aberystwyth, UK, 77 pp., 2015.

Fradkina, A. F., Grinenko, O. V., Laukhin, S. A., Nechaev, V. P., Andreev, A. A., and Klimanov, V. A.: North-eastern Asia, Cenozoic Climatic and Environmental Changes in Russia, Geol. S. Am. S., 382, 105–120, 2005.

Galbraith, R. F., Roberts, R. G., Laslett, G. M., Yoshida, H., and Olley, J. M.: Optical dating of single and multiple grains of quartz from Jinmium Rock Shelter, Northern Australia: part I, experimental design and statistical models, Archaeometry 41, 339–364, https://doi.org/10.1111/j.1475-4754.1999.tb00987.x, 1999.

Giterman, R. E., Sher, A. V., and Matthews, J. V.: Comparison of the development of tundra-steppe environments in west and east Beringia: Pollen and macrofossil evidence from key sections, Paleoecology of Beringia, Academic Press, New York, USA, 43–73, 1982.

Goslar, T., Czernik, J., and Goslar, E.: Low-energy ^{14}C AMS in Poznan radiocarbon Laboratory, Poland, Nucl. Instrum. Meth. B, 223–224, 5–11, 2004.

Grinenko, O. V., Sergeenko, A. I., and Belolyubskyi, I. N.: Paleogene and Neogene of the North-East of Russia, Part 1. Explanatory note to the regional stratigraphic scheme of Paleogene and Neogene sediments in the North-East of Russia, Yakutsk Scientific Center Siberian Branch Russian Academy of Sciences, Yakutsk, Russia, 68 pp., 1998 (in Russian).

Gubin, S. V.: Late Pleistocene soil formations in loess-ice deposits of northeast Eurasia, doctoral dissertation, Thesis abstract (avtorreferat), Serpukhov publishing house, Pushchino, Russia, 36 pp., 1999 (in Russian).

Gundelwein, A., Müller-Lupp, T., Sommerkorn, M., Haupt, E. T., Pfeiffer, E. M., and Wiechmann, H.: Carbon in tundra soils in the Lake Labaz region of arctic Siberia, Eur. J. Soil Sci., 58, 1164–1174, 2007.

Günther, F., Grosse, G., Wetterich, S., Jones, B. M., Kunitsky, V. V., Kienast, F., and Schirrmeister, L.: The Batagay mega thaw slump, Yana Uplands, Yakutia, Russia: Permafrost thaw dynamics on decadal time scale. Abstract, Past Gateways, III interna-

tional Conference and Workshop, 18–22 May 2015, Potsdam, Germany, 2015.

Harris, I., Jones, P. D., Osborn, T. J., and Lister, D. H.: Updated high-resolution grids of monthly climatic observations – the CRU TS3.10 Dataset, Int. J. Climatol., 34, 623–642, https://doi.org/10.1002/joc.3711, 2014.

Hoefs, J. and Hoefs, J.: Stable isotope geochemistry, Vol. 201, Springer, Berlin, Germany, 1997.

Ivanova, R. N.: Record low air temperatures of Eurasia, Bulletin of North-East Federal University in Yakutsk, 3, 13–19, 2006 (in Russian).

Jakobsson, M.: The International Bathymetric Chart of the Arctic Ocean (IBCAO) Version 3.0, Geophys. Res. Lett., 39, L12609, https://doi.org/10.1029/2012GL052219, 2012.

Kaplina, T. N.: History of permafrost of north Yakutia in Late Cenozoic, Nauka, Moscow, Russia, 153–181, 1981 (in Russian).

Kaplina, T. N.: Ancient alas complexes of northern Yakutia (Part 1), KriospheraZemli, XV, 2, 3–13, 2011 (in Russian).

Kaplina, T. N. and Sher, A. V.: Cryogenic structure, sedimentation and age of alluvial strara of Sypnoi Yar, Indigirka River, Permafrost and snow cover, Nauka, Moscow, Russia, 27–41, 1977 (in Russian).

Kaplina, T. N., Giterman, R. E., Lachtina, O. V., Abrashov, V. A., Kiselev, S. V., and Sher, A. V.: Duvanny Yar – a key section of the upper Pleistocene sediments on Kolyma Lowland, Bulletin of Quaternary Res. Commission, 48, 49–65, 1978 (in Russian).

Kaplina, T. N., Sher, A. V., Giterman, R. E., Zazhigin, V. S., Kiselev, S. V., Lozhkin, A. V., and Nikitin, V. P.: Key section of Pleistocene deposits on the Allaikha River (lower reaches of the Indigirka), Bulletin of Commission on Quaternary Period research, USSR Academy of Sciences, 50, 73–95, 1980 (in Russian).

Katasonov, E. M.: Litologia chetvertichnykh otlozheniy Yanskoy primorskoy nizmennosti (1954), republished in Moscow University Press, Moscow, Russia, 176 pp., 2009 (in Russian).

Katasonov, E. M., Ivanov, M. S., and Pudov, G.: Structure and absolute geochronology of alas deposits in Central Yakutia, Nauka, Novosibirsk, Russia, 95 pp., 1979.

Kienast, F., Schirrmeister, L., Siegert, C., and Tarasov, P.: Palaeobotanical evidence for warm summers in the East Siberian Arctic during the last cold stage, Quaternary Res., 63, 283–300, 2005.

Kienast, F., Wetterich, S., Kuzmina, S., Schirrmeister, L., Andreev, A. A., Tarasov, P., Nazarova, L., Kossler, A., Frolova, L., and Kunitsky, V. V.: Paleontological records indicate the occurrence of open woodlands in a dry inland climate at the present-day Arctic coast in western Beringia during the Last Interglacial, Quaternary Sci. Rev., 30, 2134–2159, 2011.

Kondratjeva, K. A.: Novie dannye obobnazhenii Mus-Khaya na reke Yana, Merzlotnye issledovaniya, 14, 56–66, 1974 (in Russian).

Konishchev, V. N.: Formation of Disperse Composed Deposits of the Cryolithophere, Nauka, Novosibirsk, Russia, 198 pp., 1981 (in Russian).

Konishchev, V. N.: The nature of cyclic structure of the Ice Complex, East Siberia, Kriosphera Zemli, XVII, 1, 3–16, 2013 (in Russian).

Konishchev, V. N. and Rogov, V. V.: Investigations of cryogenic weathering in Europe and Northern Asia, Permafrost Periglac., 4, 49–64, 1993.

Köppen, W.: The thermal zones of the earth according to the duration of hot, moderate and cold periods and to the impact of heat on the organic world, translated by: Volken, E. and Brönnimann, S., Meteorol. Z. (published 2011), 20, 351–360, 1884.

Kostyukevich, V. V.: A regional geochronological study of late Pleistocene permafrost, Radiocarbon, 35, 477–477, 1993.

Krbetschek, M. R., Götze, J., Dietrich, A., and Trautmann, T.: Spectral information from minerals relevant for luminescence dating, in: Review on luminescence and electron spin resonance dating and allied research, edited by: Wintle, A. G., Radiat. Meas., 27, 695–748, https://doi.org/10.1016/S1350-4487(97)00223-0, 1997.

Kreutzer, S., Schmidt, C., Fuchs, M. C., Dietze, M., Fischer, M., and Fuchs, M.: Introducing an R package for luminescence dating analysis, Ancient TL, 30, 1–8, 2012.

Kudryavtseva, V. A.: General Permafrost Science, Moscow University Press, Moscow, Russia, 148–171, 1978 (in Russian).

Kunitsky, V. V.: Cryolithology of the Lower Lena, Permafrost Institute Press, Yakutsk, Russia, 162 pp., 1989 (in Russian).

Kunitsky, V. V., Schirrmeister, L., Grosse, G., and Kienast, F.: Snow patches in nival landscapes and their role for the Ice Complex formation in the Laptev Sea coastal lowlands, Polarforschung, 70, 53–67, 2002.

Kunitsky, V. V., Syromyatnikov, I. I., Schirrmeister, L., Skachkov, Yu. B., Grosse, G., Wetterich, S., and Grigoriev, M. N.: Ice-rich and thermal denudation in the Batagay area (Yana upland, East Siberia), Kriosphera Zemli, XVII, 1, 56–68, 2013 (in Russian).

Larionov, P. D.: Ecological survey of a Yakutian long tail ground squirrel (Citellus eversmanni jacutensis Brandt), Zoological magazine, XXII, 4 234—246, 1943.

Lavrushin, Yu. A.: Stratigraphia i nekotorye osobennosti formirovania chetvertichnykh otlozhenij nizovjev reki Indigirki, Izvestia Akademii Nauk, Seria geologicheskaya, 2, 73–87, 1962 (in Russian).

Lavrushin, Yu. A.: Alluvium of plain rivers of subarctic zone and periglacial areas of continental glaciation, Proceedings of the Institute of Geological Sciences of the USSR, Vol. 87, AS USSR, Moscow, Russia, 266 pp., 1963 (in Russian).

Litt, T., Behre, K.-E., Meyer, K.-D., Stephan, H.-J., and Wansa S.: Stratigraphische Begriffe für das Quartär des norddeutschen Vereisungsgebietes, Eiszeitalter und gegenwart, Quaternary Sci. J., 56, 7–65, 2007.

Lydolph, P. E.: The climate of the earth, Rowman & Littlefield Publisher, Maryland, USA, 171 pp., 1985.

MacDonald, G. M., Beilman, D. W., Kremenetski, K. V., Sheng, Y., Smith, L. C., and Velichko, A. A.: Rapid Early Development of Circumarctic Peatlands and Atmospheric CH_4 and CO_2 Variations, Science, 314, 285–288, 2006.

Markov, K. K.: Sequences of Late Cenozoic deposits "Mamontova Gora", Moscow University Press, Moscow, Russia, 198 pp., 1973 (in Russian).

Meyer, H., Dereviagin, A. Y, and Siegert, C.: Palaeoclimate reconstruction on Big Lyakhovsky Island, North Siberia – Hydrogen and oxygen isotopes in ice wedges, Permafrost Periglac., 13, 91–105, 2002.

Meyer, H., Opel, T., and Laepple, T.: Long-term winter warming trend in the Siberian Arctic during the mid-to late-Holocene, Nat. Geosci., 8, 122–125, 2015.

Murray, A. S. and Wintle, A. G.: Luminescence dating of quartz using an improved single-aliquot regenerative-dose protocol, Radiat. Meas., 33, 57–73, https://doi.org/10.1016/S1350-4487(99)00253-X, 2000.

Murray, A. S. and Wintle, A. G.: The single aliquot regeneration dose protocol: potential for improvements in reliability, Radiat. Meas., 32, 377–381, 2003.

Murton, J. B., Goslar, T., Edwards, M. E., Bateman, M. D., Danilov, P. P., Savvinov, G. N., Gubin, S. V., Ghaleb, B., Haile, J., Kanevskiy, M., and Lozhkin, A. V.: Palaeoenvironmental interpretation of Yedoma silt (Ice Complex) deposition as cold-climate Loess, Duvanny Yar, Northeast Siberia, Permafrost Periglac., 26, 208–288, 2015.

Murton, J. B., Edwards, M. E., Lozhkin, A. V., Anderson, P. M., Bakulina, N., Bondarenko, O. V., Cherepanova, M., Danilov, P. P., Boeskorov V., Goslar T., Gubin, S. V., Korzun, J., Lupachev, A. V., Savvinov, G. N., Tikhonov, A., Tsygankova, V. I., and Zanina, O. G.: Reconnaissance palaeoenvironmental study of 90 m of permafrost deposits at Batagaika megaslump, Yana Highlands, northern Siberia, XI. ICOP, 20–24 June 2016, Potsdam, Germany, 2016.

Nikolskiy P. A., Basilyan A. E., Sulerzhitsky L. D., and Pitulko V. V.: Prelude to the extinction: Revision of the Achchagyi–Allaikha and Berelyokh mass accumulations of mammoth, Quatern. Int., 219, 16–25, 2010.

Novgorodov, G. P., Grigorev, S. E., and Cheprasov, M. Y.: Prospective location of the mammoth fauna in the River Basin Yana, International Journal Of Applied And Fundamental Research, 8, 255–259, 2013.

Péwé, T. L. and Journaux, A.: Origin and character of loess-like silt in unglaciated south-central Yakutia, Siberia, U.S.S.R., Geological Survey Professional Paper 1262, Washington, DC, USA, 46 pp., 1983.

Péwé, T. L., Journaux, A., and Stuckenrath, R.: Radiocarbon dates and Late-Quaternary stratigraphy from Mamontova Gora, unglaciated Central Yakutia, Siberia, U.S.S.R., Quaternary Res., 8, 51–63, 1977.

Pisias, N. G., Martinson, D. G., Moore Jr., T. C., Shackleton, N. J., Prell, W., Hays, J., and Boden, G.: High resolution stratigraphic correlation of benthic oxygen isotopic records spanning the last 300 000 years, Mar. Geol., 56, 119–136, 1984.

Plug, L. J. and Werner, B. T.: Modelling of Ice-wedge Networks, Permafrost Periglac., 19, 63–69, 2008.

Popov, A. I.: Merzlotnye yavlenia v zemnoj kore (kriolitologia), Moscow University Press, Moscow, Russia, 303 pp., 1967 (in Russian).

Romanovskii, N. N.: Fundamentals of Cryogenesis of the Lithosphere, Moscow University Press, Moscow, Russia, 1–336, 1993 (in Russian).

Romanovskii, N. N., Hubberten, H. W., Gavrilov, A., Tumskoy, V., Tipenko, G. S., Grigoriev, M., and Siegert, C.: Thermokarst and land–ocean interactions, Laptev Sea region, Russia, Permafrost Periglac., 11, 137–152, 2000a.

Romanovskii, N. N., Gavrilov, A. V., Tumskoy, V. E., Kholodov, A. L., Siegert, C., Hubberten, H. W., and Sher, A. V.: Environmental Evolution in the Laptev Sea Region during Late Pleistocene and Holocene, Polarforschung, 68, 237–245, 2000b.

Romanovsky, V. E., Drozdov, D. S., Oberman, N. G., Malkova, G. V., Kholodov, A. L., Marchenko, S. S., Moskalenko, N. G., Sergeev, D. O., Ukraintseva, N. G., Abramov, A. A., and Gilichinsky, D. A.: Thermal state of permafrost in Russia, Permafrost Periglac., 21, 136–155, https://doi.org/10.1002/ppp.683, 2010.

Rozenbaum, G. E.: Special features of lithogenesis of the alluvial planes in the Eastern Subarctic as related to the problem of the Ice (Yedoma) Complex, Problems of Cryolithology, Vol. 9. MSU Press, Moscow, Russia, 87–100, 1981 (in Russian).

Sachs, V. N.: The Quaternary Period in the Soviet Arctic, Vodtransizdat, Leningrad, Moscow, Russia, 627 pp., 1953 (in Russian).

Schirrmeister, L., Oezen, D., and Geyh, M. A.: 230 Th/U dating of frozen peat, Bol'shoy Lyakhovsky Island (Northern Siberia), Quaternary Res., 57, 253–258, 2002.

Schirrmeister, L., Kunitsky, V. V., Grosse, G., Kuznetsova, T. V., Derevyagin, A. Y., Wetterich, S., and Siegert, C.: The Yedoma Suite of the Northeastern Siberian Shelf Region characteristics and concept of formation, Proceedings of the ninth International Conference on Permafrost, edited by: Kane, D. L. and Hinkel, K. M., University of Alaska Fairbanks, Institute of Northern Engineering, 29 June–3 July 2008, Fairbanks, USA, 1595–1601, 2008.

Schirrmeister, L., Grosse, G., Wetterich, S., Overduin, P., Strauss, J., Schuur, E. A. G., and Hubberten, H.-W.: Fossil organic matter characteristics in permafrost deposits of the Northeast Siberian Arctic, J. Geophys. Res., 116, G00M02, https://doi.org/10.1029/2011JG001647, 2011a.

Schirrmeister, L., Kunitsky, V. V., Grosse, G., Wetterich, S., Meyer, H., Schwamborn, G., Babiy, O., Derevyagin, A. Y., and Siegert, C.: Sedimentary characteristics and origin of the Late Pleistocene Ice Complex on North-East Siberian Arctic coastal lowlands and islands – a review, Quatern. Int., 241, 3–25, https://doi.org/10.1016/j.quaint.2010.04.004, 2011b.

Schirrmeister, L., Froese, D., Tumskoy, V., Grosse, G., and Wetterich, S.: Yedoma: Late Pleistocene ice-rich syngenetic permafrost of Beringia, Encyclopedia of Quaternary Science, 2nd edition, vol. 3, Elsevier, Amsterdam, the Netherlands, 542–552 , 2013.

Schwamborn, G., Schirrmeister, L., Frütsch, L., and Diekmann, B.: Quartz weathering in freeze-thaw cycles: experiment and application to the El'gygytgyn crater lake record for tracing Siberian permafrost history, Geogr. Ann. A, 94, 481–499, https://doi.org/10.1111/j.1468-0459.2012.00472.x, 2012.

Sher, A. V.: Yedoma as a store of paleo-environmental records in Beringia, Beringian Paleoenvironments Workshop, Program and Abstracts, 20–23 September 1997, Florissant, Colorado, USA, 140–144, 1997.

Sher, A. V., Kuzmina, S. A., Kuznetsova, T. V., and Sulerzhitsky, L. D.: New insights into the Weichselian environment and climate of the East Siberian Arctic, derived from fossil insects, plants, and mammals, Quaternary Sci. Rev., 24, 533–569, 2005.

Siegert, C., Stauch, G., Lehmkuhl, F., Sergeenko, A., Diekmann, B., Popp, S., and Belolyubsky, I. N.: Razvitie olodenenija Verkhoyanskogo Khrebta i ego predgorij v Pleistocene: rezultaty novykh issledovanij, Regional Geology and Metallogeny, 30–31, 222–228, 2007 (in Russian).

Siegert, C., Kunitsky, V., and Schirrmeister, L.: Otlozheniya ledovogo kompleksa – archiv dannykh dlya reconstruccii climata i ecologii na poberezh'e morya Laptevykh v pozdnem Pleis-

tocene, Moscow University Press, Moscow, Russia, 320–331, 2009 (in Russian).

Slagoda, E. A.: Cryolithogenic Deposits of the Laptev Sea Coastal Plain: Lithology and Micromorphology, Publishing and Printing Center Express, Tyumen, Russia, 119 pp., 2004 (in Russian).

Strauss, J., Schirrmeister, L., Grosse, G., Wetterich, S., Ulrich, M., Herzschuh, U., and Hubberten, H.-W.: The deep permafrost carbon pool of the Yedoma region in Siberia and Alaska, Geophys. Res. Lett., 40, 6165–6170, https://doi.org/10.1002/2013GL058088, 2013.

Tarasov, P. E., Andreev, A. A., Anderson, P. M., Lozhkin, A. V., Leipe, C., Haltia, E., Nowaczyk, N. R., Wennrich, V., Brigham-Grette, J., and Melles, M.: A pollen-based biome reconstruction over the last 3.562 million years in the Far East Russian Arctic – new insights into climate–vegetation relationships at the regional scale, Clim. Past, 9, 2759–2775, https://doi.org/10.5194/cp-9-2759-2013, 2013.

Tomirdiaro, S. V.: Evolution of lowland landscapes in northeastern Asia during late Quaternary time, Paleoecology of Beringia, Academic Press, New York, USA, 29–37, 1982.

Tomirdiaro, S. V. and Chernenky, V. I.: Cryogenic deposits of East Arctic and Sub Arctic, AN SSSR Far-East-Science Center, Kriosfera Zemli, Novosibirsk, Russia, 1–196, 1987 (in Russian).

Tomirdiaro, S. V., Chernenky, B. I., and Bashlavin, D. K.: The Sypnoi Yar – a key-section of periglacial alluvial and aeolian sands of the north-east of the USSR, Stratigraphy and paleogeography of the Late Cenozoic of the Eastern USSR, Magadan, Russia, 67–79, 1983 (in Russian).

Tumskoy, V. E.: Osobennosti kriolitogeneza otlozhenii severno Yakutii v srednem Neopleistotsene – Golotsene (Peculiarities of cryolithogenesis in northern Yakutia from the Middle Neopleistocene to the Holocene), Kriosfera Zemli, Novosibirsk, Russia, 16, 12–21, 2012 (in Russian).

USSR Climate Digest: Yakutskaya ASSR, Meteorologicheskie dannye za otdelnie gody. Chast 1. Temperatura vozdykha/Red.vyp. Izjymenko S.A., Issue 24, Yakutskij gidrometeorologicheskij zentr, Yakutsk, Russia, 544 pp., 1989.

Vdovina, L. G.: Geological map of Russian Federation, scale 1 : 200 000, VSEGEI publishing house, Saint-Petersburg, Russia, 2002.

Voeikov Main Geophysical Observatory: Climatic Atlas of Asia (Goscomgidromet USSR, Gidrometeoizdat, 1981), UNESCO, WMO, Leningrad, Russia, 1981.

Walter, K. M., Zimov, S. A., Chanton, J. P., Verbyla, D., and Chapin III, F. S.: Methane bubbling from Siberian thaw lakes as a positive feedback to climate warming, Nature, 443, 71–75, 2006.

Waters, M. R., Forman, S. L., and Pierson, J. M.: Diring Yuriakh: A lower paleolithic site in central Siberia, Science, 275, 1281–1284, 1997.

Wetterich, S., Kuzmina, S., Andreev, A. A., Kienast, F., Meyer, H., Schirrmeister, L., Kuznetsova, T., and Sierralta, M.: Palaeoenvironmental dynamics inferred from late Quaternary permafrost deposits on Kurungnakh Island, Lena Delta, northeast Siberia, Russia, Quaternary Sci. Rev., 27, 1523–1540, 2008.

Wetterich, S., Schirrmeister, L., Andreev, A. A., Pudenz, M., Plessen, B., Meyer, H., and Kunitsky, V. V.: Eemian and Late Glacial/Holocene palaeoenvironmental records from permafrost sequences at the Dmitry Laptev Strait (NE Siberia, Russia), Palaeogeogr. Palaeocl., 279, 73–95, 2009.

Wetterich, S., Rudaya, N., Andreev, A. A., Opel, T., Schirrmeister, L., Meyer, H., and Tumskoy, V.: Ice Complex formation in arctic East Siberia during the MIS3 Interstadial, Quaternary Sci. Rev. 84, 39–55, https://doi.org/10.1016/j.quascirev.2013.11.009, 2014.

White, R. E.: Principle and Practice in Soil Science, Blackwell, Malden, Mass., USA, 266 pp., 2006.

Yershov, E. D. and Williams, P. J.: General geocryology, Cambridge university press, Cambridge, UK, 580 pp., 2004.

Zanina, O. G.: Cryolithic parameters and biogeographic features of soils in the Kolyma lowland during the Late Pleistocene, Geography and geoecology, Faculty of Geography Moscow State University, Moscow, Russia, 61–74, 2006 (in Russian).

Zimov, S. A., Zimov, N. S., Tikhonov, A. N., and Chapin III, F. S.: Mammoth steppe: a high-productivity phenomenon, Quaternary Sci. Rev. 57, 26–45, https://doi.org/10.1016/j.quascirev.2012.10.005, 2012.